Lecture 11 on, Landscape Micrometeorology: Integrating or Scaling Information from Canopy to Landscape Scales, part 1

April 11, 2014

ESPM 228
Advanced Topics on Biometeorology and Micrometeorology

Dennis Baldocchi
Professor of Biometeorology
Ecosystem Science Division
Department of Environmental Science Policy and Management
130 Mulford Hall
University of California, Berkeley
Berkeley, CA 94720
baldocchi@berkeley.edu
510-642-2874

http://nature.Berkeley.edu/biometlab/espm228

Outline

A. Flux Footprint Modeling
B. Spatial scaling
    1. checkerboard averaging problem
    2. Aggregration of fluxes versus resistances
    3. Data, Analysis and Measurements
    4. Satellite Information, estimating regional fluxes
    5. Wet/Dry DaisyWorld and Sub Grid Variability

Flux and Concentration Footprints

One of the most fundamental questions one can ask a meteorologist measurement fluxes at a solitary tower is: where is the flux coming from? This question is especially pertinent when one attempts to make flux measurements over small agricultural paddocks, or in the natural environment where the upwind vegetation can vary with distance and wind direction. Ironically, no one attempted to address this fundamental question until the late 1980s and early 1990s. Pioneering studies on footprint distributions and characterizations are attributed to Schuepp et al. (Schuepp et al., 1990) and Leclerc and Thurtell (Leclerc and Thurtell, 1990). In the past decade, the field of footprint modeling has matured to point that several excellent and thorough reviews exist for reference (Foken and Leclerc, 2004; Schmid, 2002; Vesala et al., 2008).

The flux footprint can be defined as (Schuepp et al., 1990):

> 'contribution per unit surface flux, of each unit element of upwind surface area to the measured vertical flux at a point'

$$F = \int_S f(s)Q(s)ds$$

In other words the flux density, F, is a spatial integral of the upwind Source-Sink function, Q, weighted by the probability function, f, that particles emitted from some incremental area, s, will be sensed at the downwind location where F is being measured.

There are two ways to examine the spatial dimension of a 'flux footprint'. One approach uses analytical, Eulerian diffusion models (Horst and Weil, 1992; Schmid, 1994; Schuepp et al., 1990). These tend to be based on the advection-diffusion equation and the Gaussian plume model. The other approach uses Lagrangian random walk models ((Baldocchi, 1997; Horst and Weil, 1992; Kljun et al., 2004; Leclerc and Thurtell, 1990).

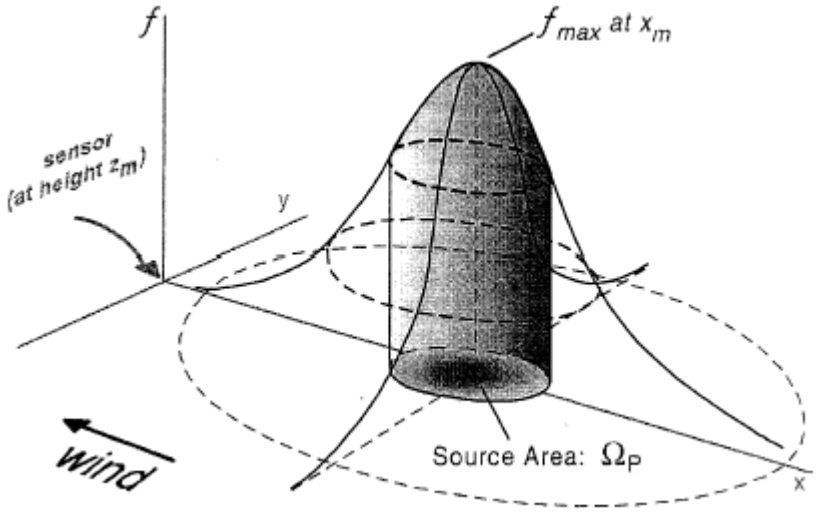

Figure 1 After Schmid, 2002

At present footprint models have been used to assess 'flux footprints' in the surface boundary layer *above* vegetation, across horizontal inhomogeneities (Luhar and Rao, 1994) and under forests (Baldocchi, 1997). Tests of the methods have been rare and are attributed to studies by Hsieh et al. (Hsieh et al., 2000a) and Leclerc et al. (Leclerc et al., 2003a; Leclerc et al., 2003b).

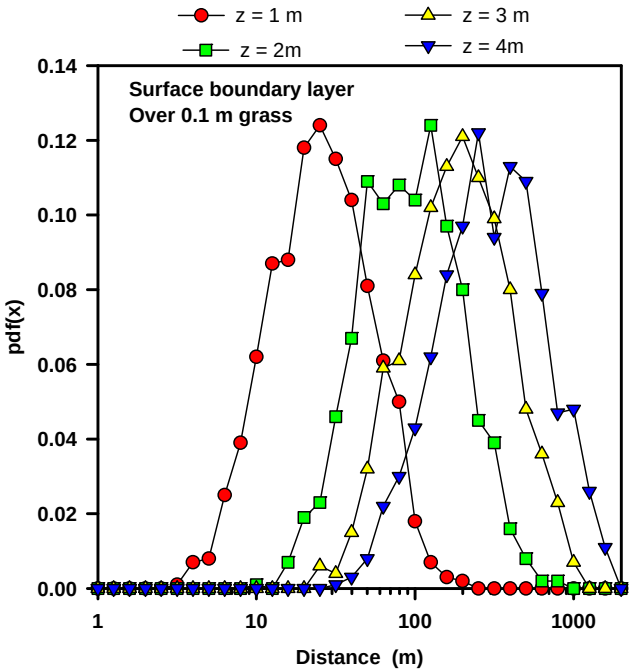

The study of footprints has much application to contemporary Biometeorology. Many micrometeorological field sites possess stands of mixed species or are over a variegated landscape. Consequently, the potential net flux at a given site will be a factor of wind direction. Until now most research teams simply sum measurements with time to assess annual net ecosystem CO2 exchange, regardless of the vegetation in different wind sectors, yielding a potential source of bias error when comparing flux tower information with fluxes derived from a grid surrounding the tower via models or remote sensing (Chasmer et al., 2011; Gockede et al., 2004; Kim et al., 2006; Rebmann et al., 2005).

We identify four problems and one issue that relate to footprints, spatial distribution of vegetation and net ecosystem CO_2 exchange. The first problem relates to the representativeness of the integrated tower record. The second problem relates to the appropriateness of conventional gap filling that does not consider the effects of wind direction on algorithm development. The third problem relates to using tower data to assess spatially integrated fluxes, as will be assessed with models and satellite information. The fourth problem relates to the definition of flux footprints with dual sources.

Problem 1: How Representative is net ecosystem-atmosphere CO2 exchange Summed From a Single Tower.

At numerous AmeriFlux sites species composition varies with wind direction (see Figure 1, Walker Branch Watershed, Oak Ridge, TN).

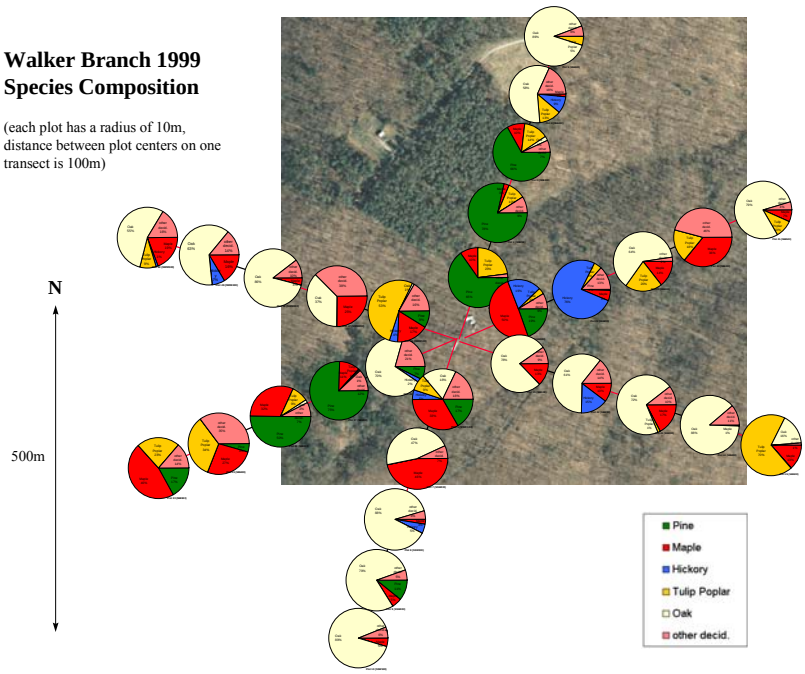

Figure 2 Analysis by Falge, data of Falge and Shindler

Hence, there is a potential to observe different carbon fluxes under identical climate conditions from different wind directions.

Because wind direction climatology (wind rose) is not uniform and is unique to each site, tailored gap filling algorithms should be developed and be applied. This leads us to problem Two.

Problem 2: Assessing the appropriateness of gap filling methods that do and do not consider the effects of wind direction on algorithm development.

In the Southeast, during the summer growing season, northeasterly winds are associated with drier conditions and clearer skies, while southeasterly winds are more humid and have billowy convective clouds. Canopy CO2 exchange is a function of sunlight, direct/diffuse radiation, temperature and humidity deficits, when soil moisture is ample. Based on these arguments alone one can expect different fluxes from different wind

directions even if the vegetation was azimuthally symmetrical. And of course many sites have varying distributions of species, as figure 1 shows.

If we are to compute the true expected value of net ecosystem CO2 exchange we test if the temporally integrated flux equals the flux weighted by wind direction:

Problem 3: How can we use tower data to assess spatially integrated fluxes the would be assessed with models and satellite information.

We cannot expect to measure fluxes at a tower 24 hours a day. Plus the tower sites are discretely spaced. Ultimately models and satellite information will be used to assess landscape scale fluxes. To do so requires summing the computed flux for each pixel. But to test and validate such a model requires that on weight model calculations with the flux footprint and the vegetation in that footprint, so the predicted model value can be represented by the flux that is measured.

One important issue is to examine wind roses at different sites and species transects to compute footprint climatologies (Amiro, 1998).

The challenge to answering some of the annotated footprint problems is to measure the flux, F, and the footprint distribution, f, and invert the integral and solve for Q across the domain of the landscape and then integrate Q spatially.

$$F = \int_S f(s)Q(s)ds$$

1. Footprint based on Analytical Diffusion Models

The flux footprint is equal to the spatial distribution of the vertical flux downwind of a unit point source located on the surface (Horst and Weil, 1992). In other words, the total flux footprint (m^{-2}) measured at a level, z_m, is related to the integral of the product of surface emission function, Q, and the footprint distribution function, f, a conditional probability function:

$$F(x, y, z_m) = \int_{-\infty}^{\infty} \int_{-\infty}^{x} Q(x', y', z = 0) f(x - x', y - y', z_m) dx' dy'$$

Inverting this equation and solving for Q will convert the measured eddy covariance flux and the flux footprint information into the grid-averaged value that is detected by models and remote sensing methods.

Analytical solutions to this relation are based on several assumptions:

1. Turbulent transfer is computed with K theory
2. There is negligible streamwise diffusion
3. The system can be represented as a two dimensional advection diffusion problem
4. Turbulent flow is horizontally homogeneous

Gash

The flux measured at a specific height, zm, at some horiztonal position, x is simply a function of the integral of the product of the source strength (mol m^{-2} s^{-1}; g m^{-2} s^{-1}) and the flux footprint distribution function f(x,z):

$$F(x, z_m) = \int_{-\infty}^{x} Q(x) f(x, z_m) dx$$

The scalar source field is defined as:

Q(x) =0, x< 0
Q(x)=Q_0; x>=0

Gash employed a solution to the two dimensional advection/diffusion equation:

$$\overline{u}\frac{\partial \overline{C}}{\partial x} = -\frac{\partial \overline{F}}{\partial z}$$

to arrive at an equation that described the fetch requirement to achieve a specified value of the normalized flux (F(x,z)/Q_0):

$$x_{fetch} = -\frac{U z_m}{k u_*} \frac{1}{\ln(F / S_0)}$$

The plume-weighted wind speed is defined as:

$$U = \frac{\int_{d+z_0}^{z_m} u(z) dz}{\int_{d+z_0}^{z_m} dz} = \frac{u_*}{k}[\ln(\frac{z_m}{z_0}) - 1 + \frac{z_0}{z_m}]$$

and is valid for neutral thermal stratification and canopies with negligible zero-plane displacement.

With the equations at hand, an expression for the normalized flux is:

$$\frac{F(x,z_m)}{Q_0} = \exp(-\frac{Uz_m}{ku_*x})$$

Substituting the first equation and solving for *f(x.z)* yields:

$$f(x,z_m) = \frac{1}{S_0}\frac{dF(x,z_m)}{dx} = \frac{Uz_m}{ku_*x^2}\exp(-\frac{Uz_m}{ku_*x})$$

This simple equation will not be appropriate during non-neutral thermal stratification, across edges with distinct changes in roughness and source strength and over tall canopies with a substantial zero-plane displacement. But it gives one insight on the methodology and logic.

The following schematic illustrates the footprint distribution function for a standard case, U/u* equal 8. For the one meter measurement height, 98% of the flux is measured within

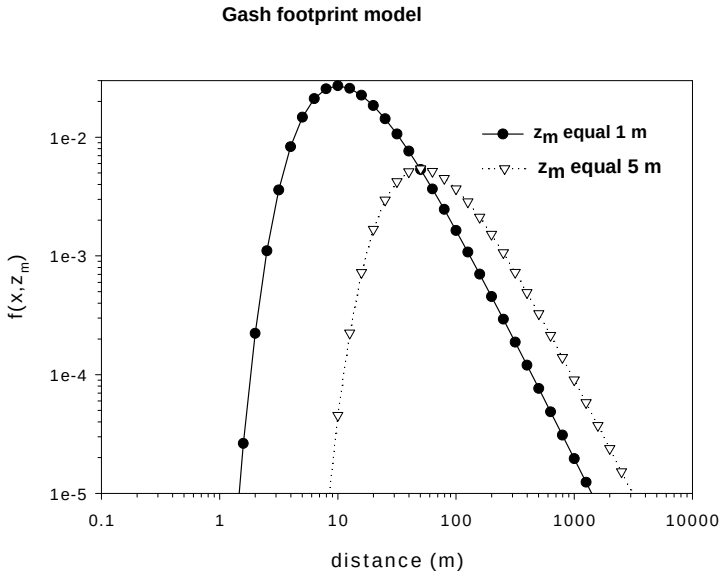

1000 m.

Schuepp et al.

Schuepp et al. expanded on the theory of Gash and developed a footprint model for a wider range of canopy and measurement heights, roughness lengths and zero plane displacements.

Schuepp starts with a relation for the concentration at a point that evolves from the release of an infinite cross wind line source in a uniform wind field:

$$C(x,z) = \frac{Q_l}{ku_* x}\exp(-\frac{Uz}{ku_* x})$$

Ql is the source strength of the line source, per unit length. In this case, th weighted wind speed has been modified to consider zero plane displacements and roughness lengths:

$$U = \frac{\int_{d+z_0}^{z} u(z)dz}{\int_{d+z_0}^{z} dz} = \frac{u_*[\ln(\frac{z-d}{z_0}) - 1 + \frac{z_0}{z-d}}{k(1-\frac{z_0}{z-d})}$$

Next one computes the vertical concentration at down wind distance x integrated over all upwind line sources from 0 to x.

$$C_x(z) = \frac{Q_0}{ku_*}\int_0^x \frac{1}{x}\exp(-\frac{U(z-d)}{ku_* x})dx$$

This relation yields a profile of concentration with a definable concentration gradient:

$$\frac{dC_x(z)}{dz} = -\frac{Q_0}{ku_*(z-d)}\exp(-\frac{U(z-d)}{ku_* x})$$

Using flux-gradient theory, this relation can be used to evaluate the vertical flux at various positions:

$$F_z = K_c(z)\frac{dC}{dz} = ku_*(z-d)\frac{dC}{dz}$$

Schuepp defines the relative contribution to the vertical flux at height z from an infinite cross-wind line source by

$$\frac{1}{Q_0}\frac{dQ}{dx} = \frac{ku_* dC(x,z)/dz}{Q_0} = \frac{U(z-d)}{u_* kx^2}\exp(-\frac{U(z-d)}{ku_* x})$$

The relation defines the one-dimensional flux footprint. Note the similarities and differences with the equation derived by Gash.

The peak of the footprint can be evaluated by evaluated as:

$$x_{\max} = \frac{U}{u_*}\frac{(z-d)}{2k}$$

And replace x with xmax produces the footprint density at the peak:

$$\frac{1}{Q_0}\frac{dQ}{dx}|_{\max} = \frac{4u_*k}{u(z-d)}\exp(-2)$$

Hseih-Katul-Detto 2 dimensional footprint model

Hsieh and colleagues (Hsieh et al., 2000b) defined a two-dimensional footprint model that has good utility. They derived an analytical model that was derived from extensive Lagrangian computations, yielding a practical model. And later Detto et al (Detto et al., 2008), expanded the model to consider stable, neutral and unstable thermal stratification.

Hshieh et al derived a cross-wind integrated, flux footprint model. The flux, F, normalized by the source, S, at some distance x and associated with a measurement height, zm, can be expressed as:

$$F(x, z_m)/S = \exp(-\frac{1}{k^2 x} D z_u^p |L|^{1-p})$$

$$z_u = z_m(\ln(\frac{z_m}{z_0}) - 1 + \frac{z_0}{z_m})$$

$$f(x, z_m) = \frac{1}{k^2 x^2} D z_u^p |L|^{1-p} \exp(-\frac{1}{k^2 x} D z_u^p |L|^{1-p})$$

Of the variables, zm is the measurement height, z0 is the roughness length, L is the Monin-Obubukov length scale.

Parameter values for D and P as a function of thermal stratification are given in the table below:

	D	P
unstable	0.28	0.59
Near neutral	0.97	1
stable	2.44	1.33

Detto et al modified the Hsieh model to derive a two dimensional flux footprint model.

$$f(x, y, z_m) = D_y(x, y)F^y(x, z_m)$$

A lateral dispersion function is estimated as:

$$D_y(x, y) = \frac{1}{\sqrt{2\pi\sigma_y}} \exp(-\frac{1}{2}(\frac{y}{\sigma_y})^2)$$

The variable associated with the standard deviation in lateral plume size, y, is a function of the standard deviation in the lateral velocity, v:

$$\sigma_y = a_1 z_0 \frac{\sigma_v}{u_*}(\frac{x}{z_0})^{p_1}$$

Together we can define the flux probability density function, f, as:

$$F(y) = \frac{1}{k^2 x^2} D z_u^p \mid L \mid^{1-p} \exp(-\frac{1}{k^2 x} D z_u^p \mid L \mid^{1-p})$$

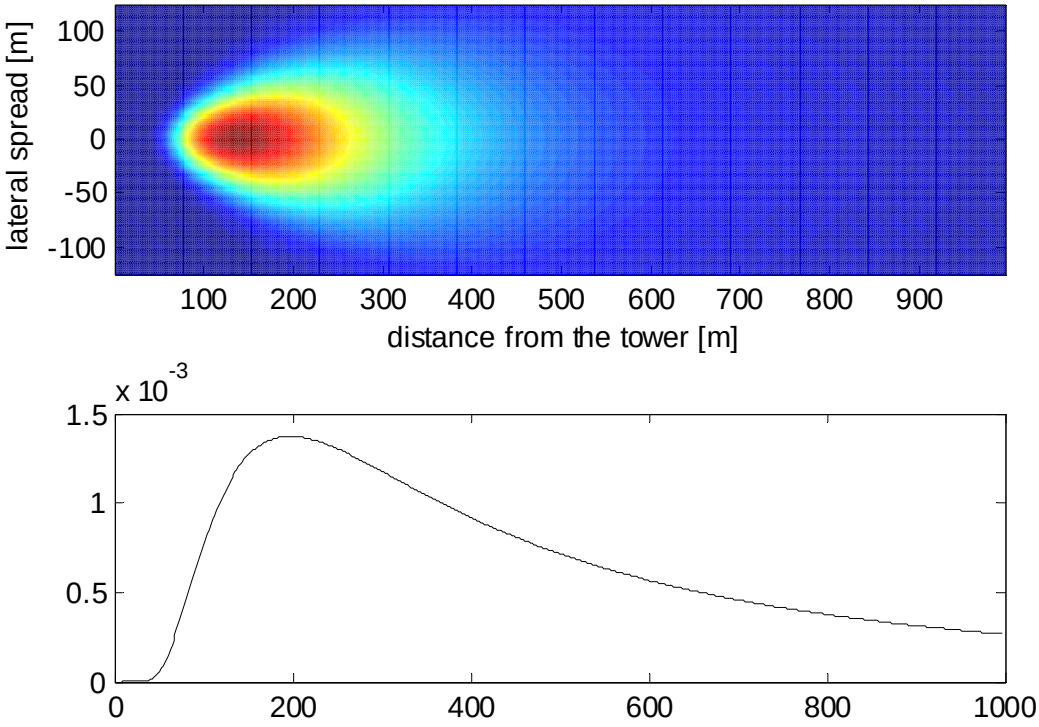

Lagrangian model

In the Lagrangian framework the flux footprint probability distribution is formally defined by a conditional probability function that the trajectory of parcels moving up and down vertically in a fluid are sensed at a location x and y and measured at point zm are defined as:

$$f(x, y, z_m) = \int_0^t \int_{-\infty}^{\infty} w(0, 0, z_m, w, t \mid x, y, z_s, t')dwdt'$$

See Rannik for definition of concentration and flux footprints

3.1.1. Forward and backward models

The conventional approach of using a Lagrangian model for footprint calculation is to release particles at the surface point source and track their trajectories downwind of this source towards the measurement location (e.g., Leclerc and Thurtell, 1990; Horst and Weil, 1992; Rannik et al., 2000). Particle trajectories and particle vertical velocities are sampled at the measurement height. In case of horizontally homogeneous and stationary turbulence, the mean concentration at the measurement location (x, y, z) due to a sustained surface source Q located at height z_0 can be described as:

$$C = \langle c(x,y,z)\rangle = \frac{1}{N}\sum_{i=1}^{N}\sum_{j=1}^{n_i}\frac{1}{|w_{ij}|}Q\left(x - X_{ij}, y - Y_{ij}, z_0\right),$$

where N is number of released particles and n_i is the number of intersections of particle trajectory i with the measurement height z; w_{ij}, X_{ij} and Y_{ij} denote the vertical velocity and the coordinates of particle i at the intersection moment, respectively. Similarly, the mean flux is given by:

$$F = \langle w(x,y,z)c(x,y,z)\rangle = \frac{1}{N}\sum_{i=1}^{N}\sum_{j=1}^{n_i}\frac{w_{ij}}{|w_{ij}|}Q\left(x - X_{ij}, y - Y_{ij}, z_0\right).$$

The concentration footprint and the flux footprint can be determined as follows:

$$f_C = \frac{1}{Q}\frac{\partial^2 C}{\partial x \partial y}, \tag{2}$$

$$f_F = \frac{1}{Q}\frac{\partial^2 F}{\partial x \partial y}.$$

Leclerc and Thurtell (Leclerc and Thurtell, 1990) used Lagrangian stochastic theory to define the probability that parcels released upwind from a source are reached by the down wind sensor. In their derivation they first defined a dimensionless form for the ratio

$$p_n = \frac{w_n}{\sigma_{wc}}$$

$$p_n = p_{n-1}\exp(-\frac{\delta t}{\tau_L(z)} + r_w\sqrt{1-\exp(-\frac{2\delta t}{\tau_L(z)})}$$

$$\delta t \le 0.1\tau_L$$

r is random number, mean of zero, variance of 1.

$$\sigma_{wc}(z) = 1.25u_*, L \ge 0$$
$$\sigma_{wc}(z) = 1.25u_*(1-4.1z/L)^{1/3}, L < 0$$

This equation is inapplicable in inhomogeneous turbulence. Wilson et al and Leclerc et al add a non dimensional drift velocity, $\frac{\overline{w}}{\sigma_{wc}} = \sigma_{wc}\tau_L\frac{d\sigma_{wc}}{dz}$

$$\frac{d\sigma_{wc}}{dz} = 0, L \ge 0$$
$$\frac{d\sigma_{wc}}{dz} = -\frac{4.1\sigma_w}{3L}(1-4.1\frac{z}{L})^{-2/3}, L < 0$$

$$z_n = z_{n-1} + \sigma_{wc}\delta t(p_n + \frac{\overline{w}}{\sigma_{wc}})$$

Be careful and generation of random numbers. Random number generators associated with C, Fortran or Basic are very simple and may repeat after 32000 calls. When calling a

random number generator hundreds of thousands of times we need better methods. Press et al in Numerical Recipes gives alternative methods.

Others (Horst and Weil (1990), Baldocchi (Baldocchi, 1997), Hsieh et al. (Hsieh et al., 2000b) start with Thomson's random walk model

$$dw_L = a(Z, w_L)dt + (C_0\varepsilon)^{1/2} d\xi$$

Gaussian forcing term with mean of zero and variance of dt, not one!

$$dZ = w_L dt$$

$$dX = \bar{u}(Z(t))dt$$

$$a = -\frac{w_L}{\tau}$$

$$\tau = \frac{2\sigma_w^2}{C_0\varepsilon}$$

Dissipation of tke from balance between shear production and buoyant production

$$\varepsilon = \frac{u_*^3}{kz}(\phi_m - z/L)$$

Numerous particle trajectories are run. The mean ensemble concentration, c, is:

$$c(x, y) = \frac{q}{u(z)} p_z(z - z_s; x - x_s)$$

q is the line source strength, pz is the pdf of the particle height and the subscript s denotes the source coordinates. Typically 5000 or more particles are released.

$$\overline{F_x} = \int_0^{x_m} F(x, z_m)dx$$

$$q = \overline{F_x} + \int_0^{z_m} \bar{u}(z)c(x_m, z)dz$$

Forest Floor Footprints

Until 1997, footprint theories in the literature were for surface layer meteorology. The assumed the vegetation to act as a single flat layer. At this juncture, the results from 'flux footprint' studies conducted in the surface boundary layer cannot be applied to the circumstance below vegetation. This restriction is imposed because the velocity, time and length scales of turbulence are heterogeneous below the canopy-atmosphere interface and differ from those measured in the surface boundary layer (Raupach, 1988; Wilson, 1989; Raupach et al., 1996; Finnigan and Brunet, 1995). For example, the standard deviation of vertical velocity (σ_w) above vegetation is about 1.25 times friction velocity, under neutral thermal stratification, while below canopy height, this metric decreases quasi-linearly with depth. Typical values for σ_w, near the soil and under vegetation, range between 15 and 40 % of the quantity measured in the surface boundary layer (Amiro, 1990; Finnigan and Brunet, 1995 ; Raupach et al., 1996;). The mean horizontal wind velocity (U) also decreases markedly with depth into a plant canopy (Raupach, 1988 ; Raupach et al., 1996). The vertical profile of wind velocity is often modeled as an exponential function of depth into the canopy (Cionco, 1965). In contrast, the mean horizontal wind profile, above a plant stand, adheres to a logarithmic wind law (Kaimal and Finnigan, 1994) and is a function of the zero plane displacement, roughness length, and Monin-Obukhov length scale. The magnitude of turbulence intensity (the ratio between the standard deviation and the mean value of wind speed) typically exceeds 100% inside vegetation, which contrasts with values below 50% in the surface boundary layer (Baldocchi and Meyers, 1988; Raupach, 1988; Wilson, 1989). Finally, the integral turbulence time scale (T_L, the time which the velocity of fluid elements remains correlated with themselves due to the persistence of turbulent motion) is generally constant within vegetation since its constituents, the Lagrangian length scale (L_w) and σ_w, diminish with depth into the canopy (Raupach, 1988). In contrast, T_L increases with height in the surface boundary layer.

In the meantime a group of biometeorologists had started measuring fluxes in the understory of canopies (Baldocchi and Meyers, 1991; Black and Kelliher, 199x; Baldocchi et al., 2000) in order to separate the overstory and understory fluxes. Obviously, questions about the representativeness of the fluxes and where they originate arise.

Inside the canopy turbulence is heterogeneous, so the analytical models we have discussed so far will fail. We applied a Lagrangian random walk model to attact this problem.

For this application, turbulent diffusion and advection was computed in the vertical and horizontal directions, above and within a plant canopy, using a Lagrangian framework (see Durbin, 1980; Thomson, 1987 ; Raupach, 1988 ; Wilson and Sawford, 1996). Vertical displacement of fluid parcels was computed as a function of time:

$$dz = w \cdot dt \qquad (2)$$

where *w* is the Lagrangian vertical velocity and *dt* is differential time increment. Incremental changes in vertical velocity were computed with the Langevin equation, an algorithm that is weighted by a deterministic forcing (which is a function of the fluid parcel's previous velocity) and a random forcing term (Thomson, 1987):

$$dw = a(z,t,w)dt + b(z,t,w)d\xi \qquad (3)$$

The coefficients *a(z,t,w)* and *b(z,t,w)* are non-linear functions of w and are defined to account for inhomogeneous turbulence. The term $d\xi$ defines a Gaussian random forcing with a mean of zero and a variance of *dt*.

The terms *a(z,t,w)* and *b(z,t,w)* are derived from the budget equation for the Eulerian probability density function of *w* (the Fokker-Planck equation) (Thomson, 1987). For the one-dimensional case, where velocity fluctuations and gradients occur only in the vertical direction, equation 3 becomes:

$$dw = (-\frac{w_L}{T_L} + \frac{1}{2}\left[1 + \frac{{w_L}^2}{\sigma_w^2}\right]\frac{\partial\sigma_W^2}{\partial z})dt + \sqrt{\frac{2\sigma_W^2}{T_L}}d\xi \qquad (4)$$

This algorithm has gained acceptance, theoretically, for it meets the model criteria proposed by Sawford (1985) and Thomson (1987), including the well-mixed criterion.

For the numerical calculations performed here, the finite difference algorithm of Luhar and Britter (1989) is used, which expresses the random operator in terms of an increment (i) that has a mean of zero and a variance of one (dΩ):

$$w_{i+1} = w_i + (-\frac{w_i}{T_L} + \frac{1}{2}\left[1 + \frac{{w_i}^2}{\sigma_w^2}\right]\frac{\partial\sigma_w^2}{\partial z})\Delta t + \sqrt{\frac{2\sigma_w^2}{T_L}\Delta t}d\Omega \qquad (5)$$

Equations 4 and 5 do not consider the impact of non-Gaussian and skewed statistical properties on the movement of fluid parcels, although these are distinct characteristics of canopy turbulence (Raupach, 1988; Wilson, 1989; Raupach et al., 1996). The rationale for neglecting the impact of non-Gaussian turbulence statistics on Equations 4 and 5 is based on information in a recent article by Wilson and Sawford (1996). They report that Lagrangian models, which considered the effect of non-Gaussion turbulence on fluid element movement, perform worse than Thomson's 1987 model, which assumes Gaussian and Eulerian turbulent statistics.

Horizontal displacements were computed for two situations. The simplest case assumed that horizontal displacements were a function of the mean, horizontal wind velocity (U):

$$dX = U(z)\cdot dt \qquad (6)$$

The second, and more complex case, considered the impact of horizontal wind velocity fluctuations (u).

$$dX = (U + u)dt \qquad (7)$$

The inclusion of *u* in Equation 7 necessitates the evaluation of Langevin model for horizontal wind velocity:

$$du = a(z,t,u)dt + b(z,t,u)d\xi \quad (8)$$

Algorithms presented in Flesch and Wilson (1992), which were derived from the theory of Thomson (1987), were used to define the coefficients *a(z,t,u)* and *b(z,t,u)*. When applying the Langevin equation to the case of two-dimensional turbulent transfer, the definition for *b* coefficient, in Equations 8 and 3, remains the same:

$$b = \sqrt{\frac{2\sigma_W^2}{T_L}} \quad (9)$$

The *a(z,t,u)* coefficient for situations where *w* and *u* fluctuations are considered, however, differs markedly from the corresponding term in Equation 4. Its derivation from the Fokker-Planck equation (Flesch and Wilson, 1992), yields a relationship that includes terms relating to the covariance between w and u (*wu*), the mean horizontal wind velocity gradient (*dU/dz*) and the standard deviation in horizontal wind velocity (σ_u):

$$a_u = \frac{1}{2(\sigma_U^2\sigma_w^2 - \overline{uw}^2)} b_u^2[\sigma_w^2 u - \overline{uww}] + \frac{1}{2}\frac{\partial \overline{uw}}{\partial z} + w\frac{\partial U}{\partial z} + \frac{1}{2(\sigma_u^2\sigma_w^2 - \overline{uw}^2)} \times\left[\sigma_w^2 \frac{\partial \sigma_u^2}{\partial z} wu - \overline{wu}\frac{\partial \sigma_u^2}{\partial z} w^2 - \overline{wu}\frac{\partial \overline{wu}}{\partial z} wu - \sigma_u^2 \frac{\partial \overline{wu}}{\partial z} w^2\right] \quad (10)$$

For the case of two-dimensional turbulent transfer, one must also re-evaluate the Fokker-Planck equation and define another algorithm for *a(z,t,w)* (see Flesch and Wilson, 1992):

$$a_w = \frac{1}{2(\sigma_U^2\sigma_w^2 - \overline{uw}^2)} b_w^2[\sigma_u^2 w - \overline{uww}] + \frac{1}{2}\frac{\partial \sigma_w^2}{\partial z} + \frac{1}{2(\sigma_u^2\sigma_w^2 - \overline{uw}^2)} \times\left[\sigma_w^2 \frac{\partial \overline{wu}}{\partial z} wu - \overline{wu}\frac{\partial \overline{wu}}{\partial z} w^2 - \overline{wu}\frac{\partial \sigma_w^2}{\partial z} wu - \sigma_u^2 \frac{\partial \sigma_w^2}{\partial z} w^2\right] \quad (11)$$

The scalar flux at a point (x,z) is calculated as:

$$F(x,z) = \frac{S_0}{N}(n\uparrow - n\downarrow)$$

$$f(x,z) = \frac{1}{S_0}\frac{dF(z,z_m)}{dx}$$

A. Model Parameterization

Within vegetation, U was computed from an exponential relation, first proposed by Cionco (1965):

$$U(z) = U(h)\exp(-\alpha(1-\frac{z}{h})) \qquad (12)$$

where h is canopy height and α is the canopy wind velocity attenuation coefficient. The attenuation coefficient typically ranges between 0.5 and 5, and tends to increase as canopy density progresses from sparse to dense (Cionco, 1978). The logarithmic wind law was applied to calculate horizontal wind velocity above the vegetation:

$$u = \frac{u_*}{k}\ln\left(\frac{z-d}{z_0}\right) \qquad (13$$

where u_* is friction velocity, k is von Karman's constant (0.4), d is the zero plane displacement height and z_0 is the roughness length. The reader should note that Equation 13 applies only for conditions of near-neutral, thermal stratification.

Within vegetation, σ_w/u_* and σ_u/u_* were approximated to decrease linearly with depth (Raupach, 1988) using:

$$\sigma_{w,u}/u_* (z) = a_0 + (a_1 - a_0)\, z/h \qquad (14$$

The coefficient, a_1, was assumed to equal 1.25 for σ_w/u_* and 2.39 for σ_u/u_*. The coefficient, a_0, ranges between 0.1 and 0.5 (Raupach, 1988). The vertical variation in the covariance between w and u (*wu*) was prescribed to decrease exponentially with depth into the canopy (Uchijima and Wright, 1964).

For most circumstances Lagrangian time scale (T_L) was assumed to be invariant with height, within vegetation (Raupach, 1988, 1989), and was approximated as:

$$T_L = 0.3\, h / u_*. \qquad (15$$

However, there are data in the literature showing T_L u*/h to be as low as 0.1 (Amiro, 1990). In the surface boundary layer T_L was approximated, under near neutral stability, as (see Raupach, 1989):

$$T_L = k\,(z-d)/(1.25\, u_*) \qquad (16$$

For the theoretical computations reported in this paper, the canopy was considered to be horizontally extensive and homogeneous and the atmosphere was assumed to have a neutral thermal stratification. Flux footprints were computed by releasing a large ensemble of fluid elements (> 5000) from the forest floor; the algorithms for parcel movement were coded in C, compiled with a 32 bit compiler, and run on a Pentium-class personal computer. The trajectory of each fluid element was tracked and the number of elements that crossed specified heights, after a given travel distance, were counted. The sum of fluid elements captured, at each bin, was normalized by the source strength. Normalization insured that the integral, with respect to distance (x) at each level, equaled one when integrated between zero and infinity.

Several boundary conditions were specified for the random walk calculations. The time step of each incremental movement was equal to 0.025 T_L(h). Fluid elements

reaching the forest floor were reflected perfectly, an *ad hoc* approach that is valid for Gaussian turbulence (Sawford, 1985; Wilson and Sawford, 1996). With regard to wind profile calculations, the zero plane displacement (d) was set at 0.6h and the roughness parameter (z_o) was 0.1h. Friction velocity was assumed to equal 0.5 m s^{-1}.

Preliminary tests, to debug the model, were made by comparing numerical calculations with output from the analytical model of Schuepp et al. (1990). For model calculations representative of the surface boundary layer, both models yielded identical horizontal positions for the peak of the source probability distribution. The numerical model, however, computed a narrower footprint source area than the analytical model. This difference is identical to results published in an earlier analysis by Horst and Weil (1992).

A comparison between Schuepps model and a random walk model based on the random walk algorithm of Thomson.

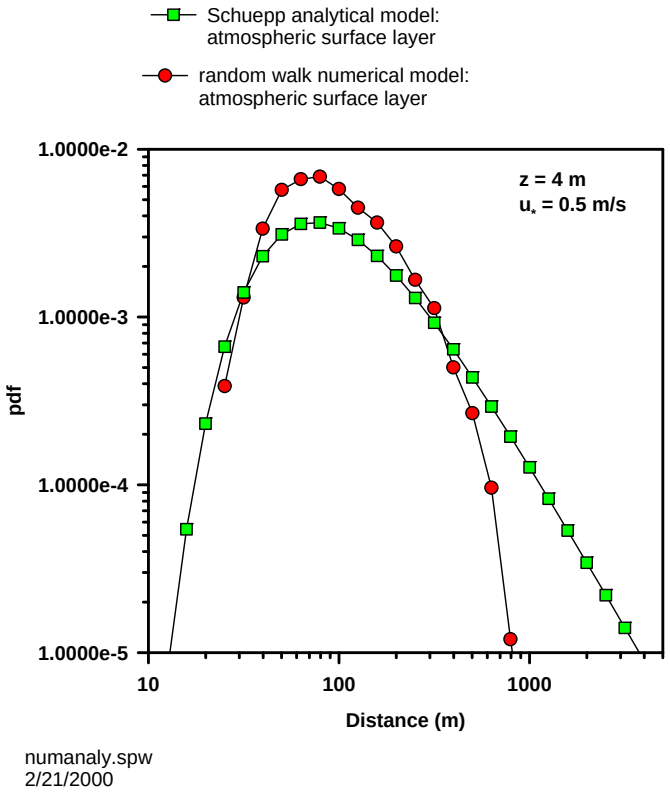

What is the characteristic of the Flux footprint over a system with separate sources or sinks, as occurs over tall canopies with distinct contributions from the soil and vegetation. Conceptually, the particle movement can be represented with figure 2.

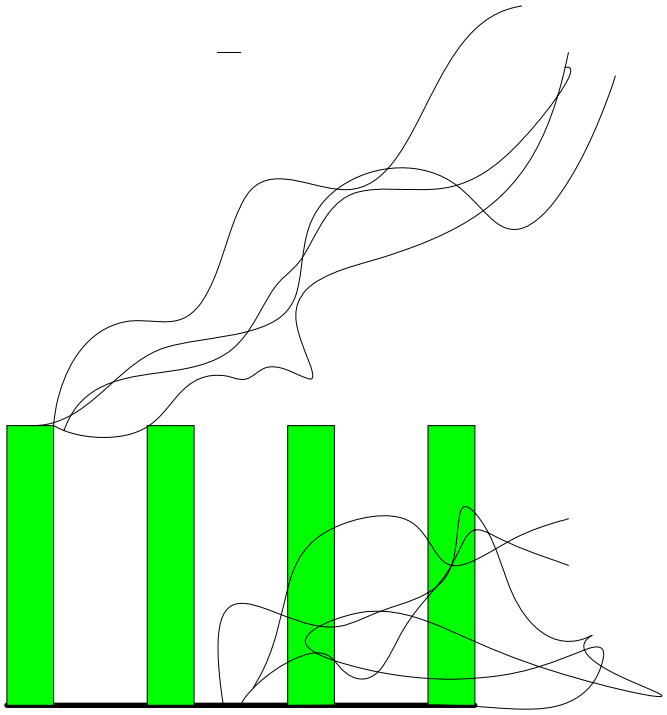

With numerical models we can investigate the role of multiple and distributed sources on the footprint. This effect has the potential to be important over tall forests

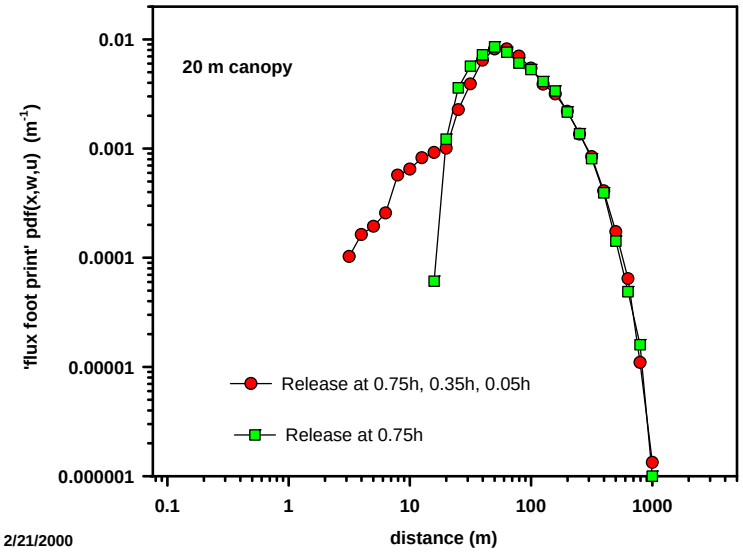

Here we see the two footprints over lap in the range between 20 and 1000 m. The impact of multiple sources is greatest only near to the source (in this case for measurements at 32 m).

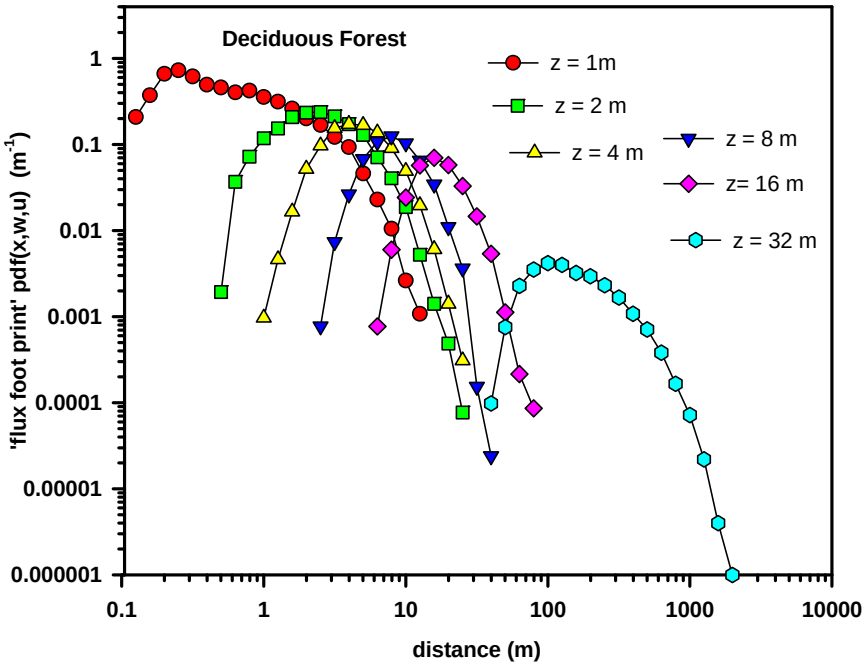

Landscape Micrometeorology

As one flies across the continent, one observes a quilt-work of land surfaces of varying size, shape and complexity. Some of the landscape patterning is artificial or aspects are natural. For example, variations in landscape composition and texture may be related to height, slope and aspect of hills and mountains. These factors have pronounced effects on the climate and soil texture and moisture, which combine to affect the sustainability or omission of certain plant types and forms. Fire and disturbance histories (floods, land slides, insect infestations etc) are other factors causing landscape complexity, as they destroy one plant group and allow another to invade and succeed. As we glide over agricultural regions, we see a mosaic of squares and circles, some green and others brown, and all changing with the seasons. Flying to the Great North, the landscape mosaic is punctuated by land and lakes, each with distinct surface properties. And finally approaching the populated regions of the country, one sees a mix of urban and suburban structures mixed with parks, tree-lined streets and yards. An example of how a complex landscape affects regional temperature and humidity can be illustrated using data from a flight pattern across a boreal landscape. Passing over lakes, aspen trees and spruce stands cause temperature and humidity to oscillate. In particular, a lake is much colder than the surrounding land.

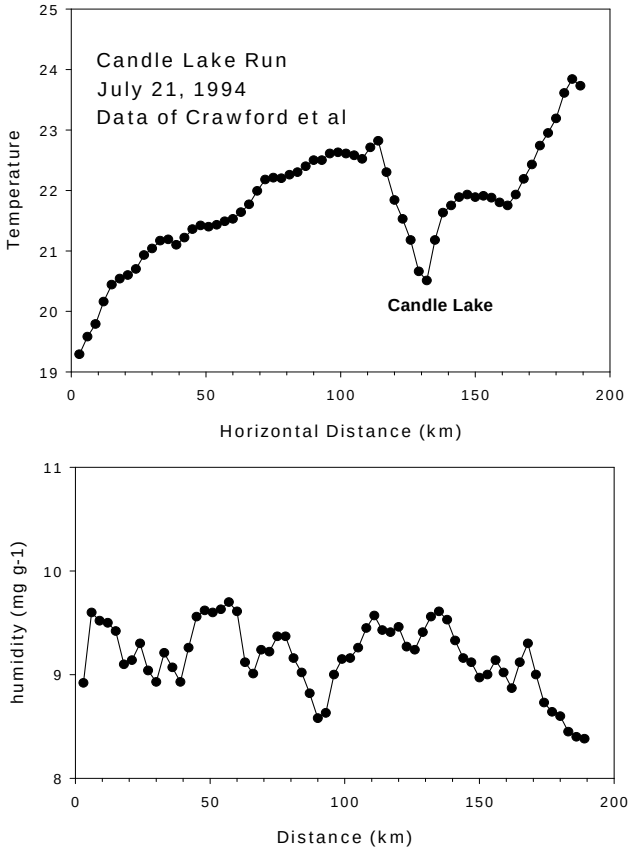

Figure 3 Aircraft transect of meteorological conditions across the southern reaches of the Boreas project. The data are from Crawford et al(Crawford et al., 1996).

How do such mosaics of land interact among themselves and with the atmosphere? This is the question addressed in this lecture. Topics involved include summing sub-grid fluxes and surface characteristics to the grid scale, the effects of advection as information is translated horizontally across landscapes, and flow over hills. This information will provide an introduction, guide and rationale for the subsequent lecture on flux footprints. It will also form a framework for understanding plant-atmosphere interactions at the regional and continental scales.

The Scaling Problem

Numerical models are atmospheric scientists' chief tool for assessing the atmosphere's weather, climate and chemistry. While models have many strengths, the parameterization of scalar fluxes at the earth's surface, the model's lower boundary condition, remains a persistent problem. Two key issues are associated with the parameterization of surface fluxes are of particular interest to micrometeorologists: One issue concerns the fidelity of the submodels to calculate scalar flux densities to and from a given patch of land

(Raupach, 1995; Shuttleworth, 1991). The second issue concerns the spatial variability of surface fluxes within and among constituent patches of a landscape and the integration of these fluxes to the scale of the model grid (Avissar, 1995; Baldocchi et al., 2005; Brunsell and Gillies, 2003)

When modeling regional and global scale problems, atmospheric modelers divide the domain into multiple cells. The horizontal length scale of individual cells typically range between 1 and 10 km on a side for mesoscale problems (Avissar and Verstraete, 1990; Pielke et al., 1998) and 100 to 500 km on a side for global problems . Landscapes, whose dimensions correspond to the grid size of a model, are rarely uniform. Typically, grid-size regions are comprised of a mosaic of land patches, each with a different potential to control or influence momentum, mass and energy transfer.

The topic of this lecture is on scaling and integrating information from a point above a canopy to the landscape. Several key scientific questions arise from this topic. If we are thinking of a top-down approach as is required by mesoscale and global modelers, the key question is what role does subgrid heterogeneity have on the grid-scale flux. Advection, flow over non-uniform terrain, subgrid averaging schemes, flux and concentration footprints and the role of interacting boundary layers must be examined. Topics discussed in this lecture and the next have relevance to problems relating to landscape ecology too.

The following figure presents an idea of an nested approach to studying a complex spatial scaling problem. The nested scale approach is an idea that has been central in the design of many international field experiments, such as FIFE (Sellers and Hall, 1992), HAPEX/MOHIBLY(Gash et al., 1989), BOREAS (Sellers et al., 1997) and BARFEX (Doran et al., 1992) and the CARBO Europe Regional study (Dolman et al., 2006) .

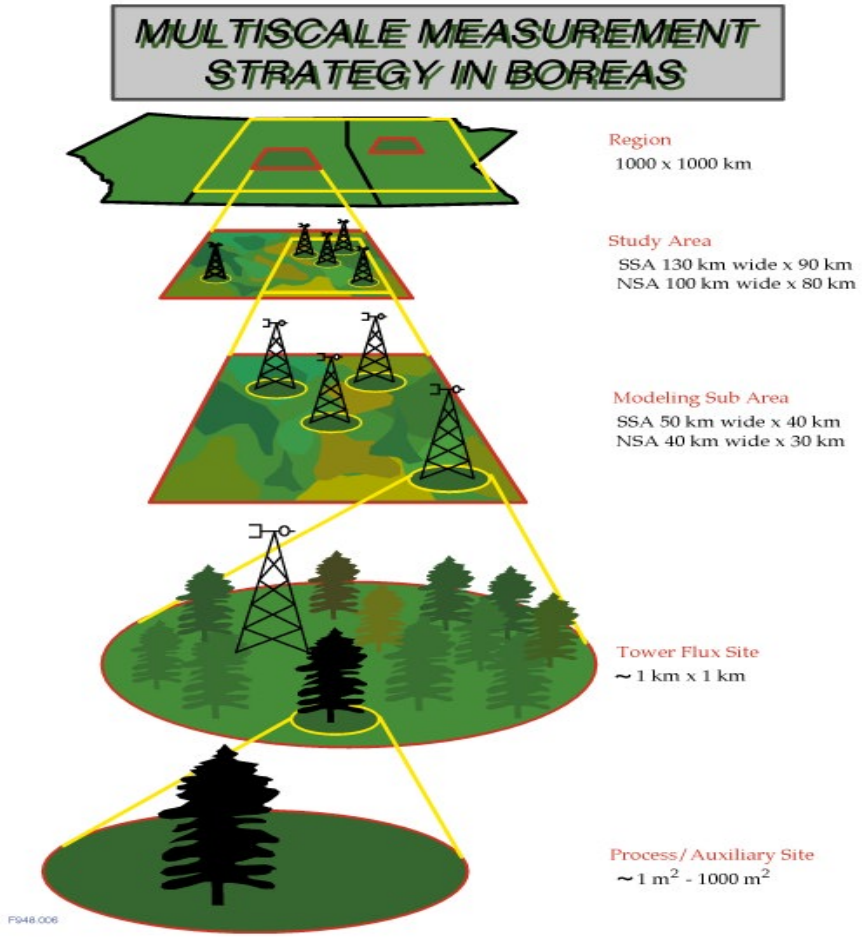

Figure 4 Nested scales of energy exchange, Boreas web page

Detailed process studies are investigated at the leaf, needle and shoot scale. This information provides an understanding of fluxes at the plant or tree scale. How plants combine, compete and shelter one another affects fluxes at the canopy scale. A collection of canopies produces landscape scale information. And finally the superpositioning of landscapes in a region add up to the size of grids in general circulation models, eg 100 km on a side.

Tools for Measurement and Analysis

There are numerous methods to assess landscape scale variability. Instruments, mounted on aircraft, are one of the best approaches (Crawford et al., 1996; Desjardins et al., 1982; Miglietta et al., 2007). Such aircraft can fly a few 10s of meters over land surfaces, measuring transects of surface fluxes, temperature, humidity and CO_2. Such platforms can also perform vertical profiles, stacked flights and long transects to assess advection, flux divergence, pbl growth and entrainment.

Remote sensing, on an aircraft or satellite platform can be used to characterize surface features and scales of variance. Boundary layer profile systems such as LIDAR, RASS, radiosondes and tethersondes can produce vertical wind, temperature and humidity

profiles through the boundary layer and produce an integrated signal of the complex lower layer.

Below is an example of an experimental aircraft used for measuring surface layer fluxes. It was developed and piloted by the late Dr. Tim Crawford. The system was able to fly at about 50 m/s and about 10 m above the surface. It carried instruments to measure position, wind velocity components, CO2, water and temperature fluctuations and remote sensing gear to assess the properties of the landscape.

Figure 5Tim Crawford's Long EZ aircraft instrumented with sensors to measure wind, turbulence, CO2, water and heat exchange.

European groups and scientists at San Diego State and NOAA/ATDD are now adopting this instrument platform on the Sky Arrow aircraft, which is available from a commercial manufacturer in Italy.

Quantitative Measures

There are numerous numerical tools for quantifying surface heterogeneity. Popular tools include semi-variograms or structure function (D), which examine the spatial variance with lag differences, h, from reference points in the scene. Below we define the structure function in terms of the expected values of the square of difference between two functional realizations separated by the distance h:

$$D_x(h) = E[(f(x+h) - f(x))^2]$$

Within the inertial subrange of turbulence the structure function scales with the 2/3 power of the separation distance, h. These functions are evaluated in an omni-directional fashion.

Spatial correlation graphs have several important characteristics that merit discussion, called the **sill, range** and the **nugget**. The sill is the value of the semi-variagram when the function reaches a constant asymptote. The distance at which the sill is attained corresponds with the range. The range denotes the scale of the variance and the sill represents the magnitude of the variance. The nugget is the variance at a lag of zero. It represents small scale variance in the scene.

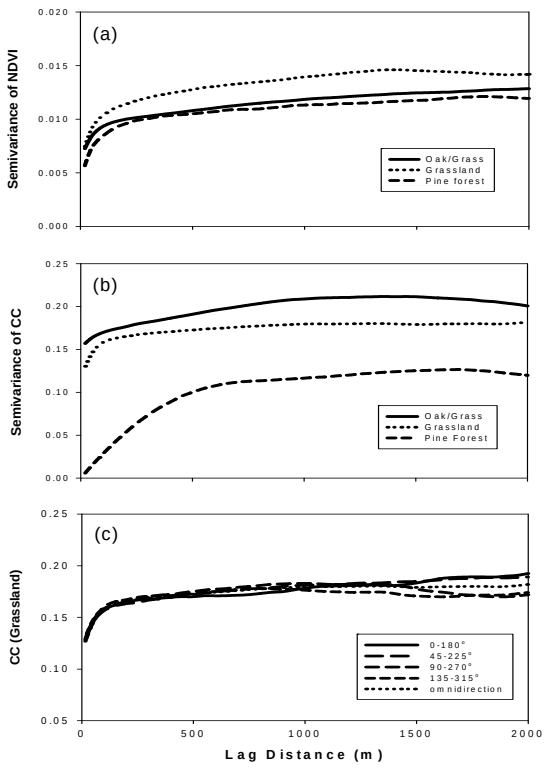

Figure 6Spatial statistics of an eddy flux field site (Kim et al., 2006)

One can also assess a related quantity, the lag-correlogram:

$$R_{yy}(\lambda) = (\Gamma \xrightarrow{\lim} \infty)\frac{1}{2\Gamma}\int_{-\Gamma}^{\Gamma} y(x)y(x+\lambda)d\lambda$$

An appeal of the lag-correlogram is that it can be expressed in terms of a Fourier transform, so the computationally efficient FFT method can be used to assess it, rather than a brute force method, as implied from above.

Sub-Grid Analysis

The process of aggregating information changes the variance of the field. We can address this question by examining a high resolution image of a landscape, as measured with the IKONOS satellite, at 4 m resolution, and compare the output with a truly artificial and random spatial field. The question to ask is how the resolution of the

averaging window alters the spatial variance, and later if this variance is averaged out will it affect the evaluation of non-linear functions, averaged over the domain?

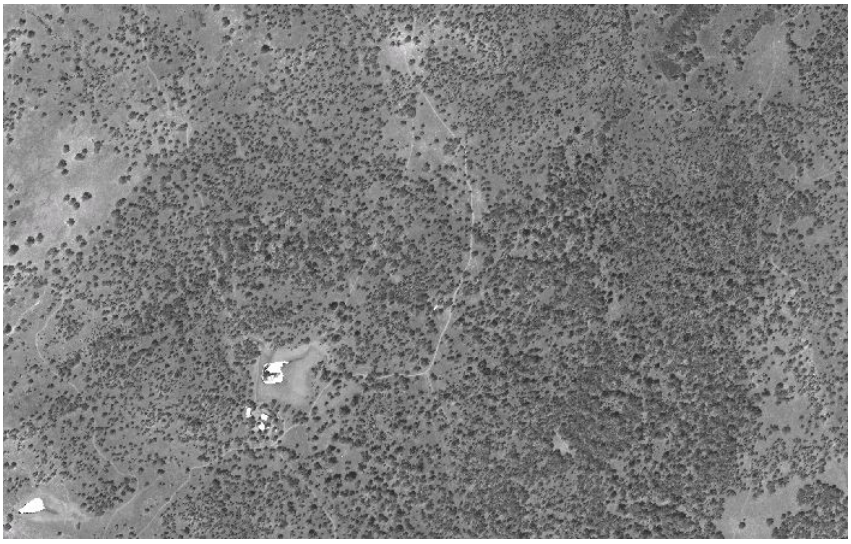

For the cases of an oak savanna in California, the variance of NDVI decreases with a -0.4 power as the window of the averaging grid increases. In contrast the slope is -1.0 if the spatial field is truly random (Levin, 1992).

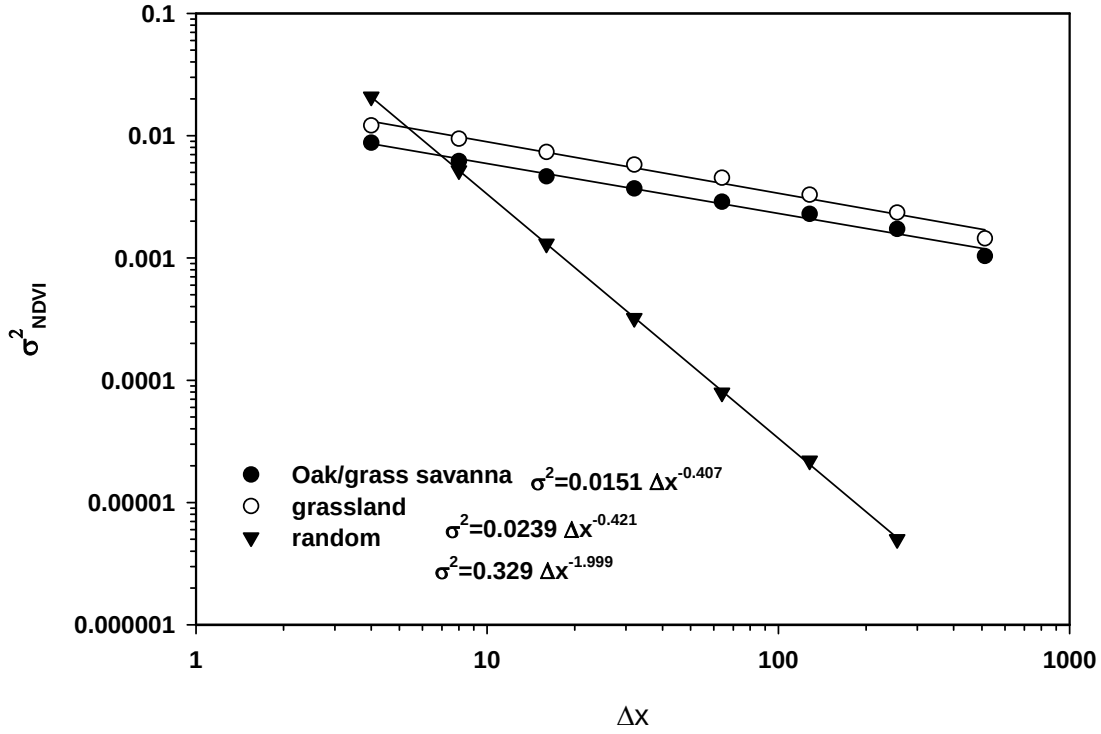

Figure 7 (Baldocchi et al., 2005)

Turbulence, Friend and Foe in Spatial Scaling?

On one hand, turbulence is chaotic and unpredictable. This feature leaves us with natural variability of fluxes and scalars that is often on the order of 10-20% over the most uniform surfaces. On the other hand, the multi-scaled nature of turbulence and its possession of large scale eddies, mixes the air well, minimizing the impact of small scale heterogeneities. Consider an open sorghum field. Within a meter we may have soil temperatures that vary by 10 to 20 C. If these differences persisted on a field scale, this temperature difference would produce a highly advective situations. But the spatial scale of difference in the crop is only 0.75 m. Horizontal gradients of temperature above the surface are much smaller (Graser et al., 1986) because eddies mix and minimize differences in air temperature that would result if the air were still.

A simple solution to averaging the effects of small scale heterogeneities is to measure surface fluxes at a higher level. Of course questions rise to how high is enough, or too much? In many past lectures we have attempted to remain within the internal boundary layer, but outside the roughness sublayer. A higher level, is the blending height. At the blending height, the impacts of each internal boundary layer are indistinguishable. Brutsaert argues that Monin Obukhov similarity theory is still valid at the blending height, as it is in the atmospheric surface layer, though it may not hold above it, as the logarithmic profiles start to deviate for ideal.

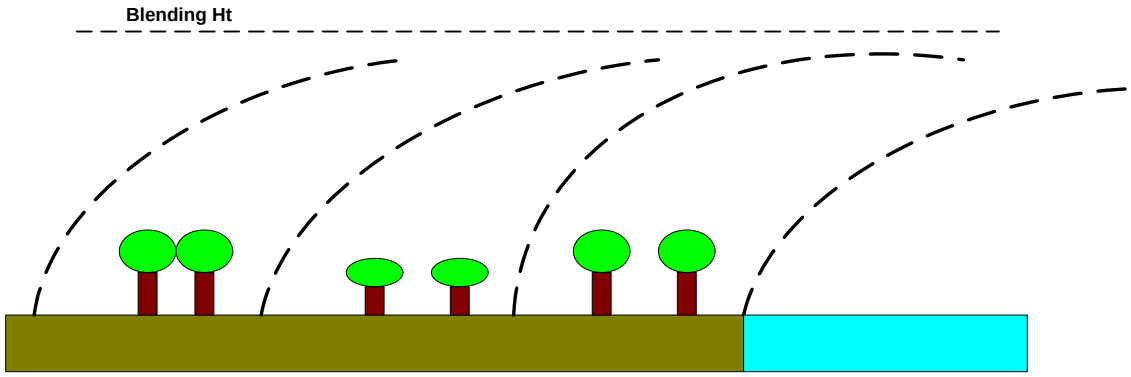

Figure 8 Overlapping surface boundary layers, merging at the blending height

Using a combination of field data and numerical calculations, several rules of thumb have been developed on when the scale of heterogeneity becomes important. Raupach (Raupach, 1991b; Raupach, 1998; Raupach and Finnigan, 1995) , using a slab model, and Avissar (Avissar, 1995; Avissar and Pielke, 1989) using a sophisticated mesoscale model, conclude that heterogeneities smooth out when the length scale is less than 5 km or they

are less than the mixing scale of the planetary boundary layer. When larger heterogeneities co-exist (> 5 km) mesoscale circulations can be established which can transport energy and cause mesoscale fluxes, which can exceed surface turbulence fluxes. Examples of this phenomenon have been observed recently by Leclerc and students, studying fluxes over forests, but downwind from clear cuts. The scale was right to generate upward motions over the clear cut and mean downward motions over the nearby forest.

Scales of variation in turbulence.

Brutsaert (1998) uses dimensional arguments to discuss the relative magnitude of horizontal and vertical scales. Vertical propagation of a smoke plume is proportional to the standard deviation of vertical velocity, horizontal propagation of the plume is proportional to the horizontal wind velocity, u., leading one to conclude:

$$\frac{dz}{dx} \sim \frac{\sigma_w}{\bar{u}}$$

These arguments lead to the ratio of length scales

$$\alpha = 0.25\left(\frac{z}{z_o}\right)^{1/7}$$

For roughness ratio of 100 to 1000, the length scale ratio is on the order of 1 to 10 (0.13 to 0.093). Brutsaert (1998) cites that this scale ratio increases to 1 to 100 as one enters the internal, equilibrium boundary layer.

Using similarity and scaling laws one can derive for non-neutral conditions:

$$\frac{dz}{dx} = \frac{1.8\left(zk\frac{g}{T}\frac{H_v}{\rho C_p}\right)^{1/3}}{\bar{u}}$$

Flux Aggregation and Averaging

Spatial variation of fluxes is ubiquitous. Studies such as the First ISLSCP Field Experiment (FIFE) suggest that that sub-grid spatial variability can be large, eg 10 to 20% for H and LE, or on the order of 20-30 Wm^{-2}.

Why is this spatial variability in energy fluxes and partitioning important? The proposed radiative forcing by doubling CO_2 is only 4 W m^{-2}. Bias errors associated with an inability to account for spatial variations in land surface properties, land surface parameterization and summation of fluxes have the potential to swamp the potential radiative forcing and the calculation of surface temperature in global models.

Faced with the complexities of the real world, how does one proceed to parameterize surface scalar flux densities and evaluate them for an entire grid? The problem we are facing in some respects is a horizontal version of the canopy integration problem we have dealt with already.

The simplest scheme for parameterizing grid scale flux densities of mass and energy involves weighting scalar flux densities from constituent patches according to their relative area (Claussen, 1991). The accuracy of this assumption is the subject of debate. When adjacent patches differ in their ability to provide moisture to the atmosphere, advection of heat and moisture can occur between fields (Baldocchi and Rao, 1995; Klaassen and Claussen, 1995; Rao et al., 1974), which is discussed in a later section.

Airplane-mounted flux systems are one means of acquiring data to evaluate parameterization schemes for spatially-averaged scalar flux densities. Yet, there remains a problem of verifying aircraft-originated flux densities for this task. The conventional approach compares aircraft-based measurements against tower-based measurements (Crawford et al., 1993; Desjardins et al., 1997).

From the airplane's perspective, airplane and tower-based flux measurement systems need not agree to verify an aircraft's flux measurement system. Towers reside in the surface layer and are immersed in a fully-developed equilibrium boundary layer, while aircraft are flying through multiple and evolving surface boundary layers (Schuepp et al., 1990). Ironically, to verify aircraft flux measurements, which are needed to address the advection problem at the regional and global model grid-scale, we must first address the advection of heat and moisture between adjacent fields at the local scale.

The issue of aggregating fluxes in landscapes to the scale of a model grid is an issue of concern because practitioners are unable to sum and average the fluxes *a priori*. Lacking information on flux they must infer the flux from parameters such as the roughness length, albedo, surface and aerodynamic conductances. But since the functions to which these variables are applied are non-linear the aggregated variables are not the proper input into the summation models, or when used additional terms must be evaluated.

For example

$$u(x,y,z) = \langle u \rangle + u''(z,y,z)$$

Let's start with sensible heat flux. We want to the expected value of heat $< H >=< \rho_a C_p \frac{(T_s - T_s)}{r_{ah}} >$, but from common field measurements we generally can only evaluate <H> in terms of mean temperatures and resistances:

$$\rho_a C_p \frac{(< T_s > - < T_s >)}{< r_{ah} >}$$

Is this correct? Taylor's Expansion gives us insight on the averaging problem. From it we can derive a relation for how the Expected value of a function compares with the function that evaluates the variable at its mean value.

$$f(x) = f(x_0) + (x - x_0)\frac{df}{dx} + \frac{(x - x_0)^2}{2!}\frac{d^2 f}{dx^2} + \frac{(x - x_0)^3}{3!}\frac{d^3 f}{dx^3} + \ldots$$

We can use the concepts from Taylor's expansion theory to evaluate expected value of non-linear functions:

$$E[f(x)] = f(\bar{x}) + \frac{1}{2}\frac{\partial^2 f(\bar{x})}{\partial x^2}\sigma_x{}^2$$

If either $\frac{1}{2}\frac{\partial^2 f(\bar{x})}{\partial x^2}$ or $\sigma(\bar{x})^2$ equal zero then $E[f(x)] = f(\bar{x})$. The first case becomes zero when the functional relationship is linear. The second term approachs zero when there is little variance

$$E[H(T_s, T_a, R_a)] = \rho_a C_p \frac{(< T_s > - < T_s >)}{< R_{ah} >} + \frac{1}{2}\frac{\partial^2 H}{\partial R_a{}^2}\sigma^2_{R_a} + \frac{1}{2}\frac{\partial^2 H}{\partial T_s{}^2}\sigma^2_{T_s} + \frac{1}{2}\frac{\partial^2 H}{\partial T_a{}^2}\sigma^2_{T_a}$$

Since *H* is a linear function of T_s and T_a, the second derivatives of those terms will go to zero. But the second partial of H with respect to Ra is proportional to

$$1/R^3{}_a$$

Conceptually, the fluxes sum and scale linearly and must be conserved, so flux weighted estimates of the resistances and driving potentials are preferred (McNaughton, 19xx). Unfortunately, we do not have flux information, but want to derive it from its components, resistances, conductances and scalar concentration measurements.

In fact addressing this question is at the heart of our work on developing a 2-d Daisy World that produces a complex 2-d pattern of soil, wet and dry vegetation, on which we can evaluate spatial integrals of fluxes and compare with the components of the spatial field. It is a way to use a known field to assess representativeness of large domains. Next year we will have computations to provide the class on this topic.

In lieu of direct simulation of subscale variability and fluxes we can use either a mosaic approach or parameterized areally averaged fluxes.

Mosaic approach: separate models are used to compute fluxes from each patch and a weighted average is used to compute the mean flux from the scene.

Parameterized Areally Averaged Flux: Less computationally demanding. Requires aerial averaging/parameterization of components.

Let's start with the definition of the expected value of a function. We need to assess the function across the variable domain, x, and know the probability density function of x.

$$E[f(x)] = \int_{-\infty}^{\infty} f(x)p(x)dx$$

The simple case of LE as a function of canopy conductance produces

$$E[\lambda E] = \frac{1}{A}\int \lambda E(G_c)dA = \int \lambda E(G_c)\,p(G_c)dG_c$$

Momentum resistance

Several approaches exist in the literature estimating an areally averaged roughness length (Garratt, 1992), since it is one of the prime factors in global circulation models and was the first problem of sub-grid variability that was faced by meteorological and climatic modelers.

One needs to define a roughness length that should produce a shear stress averaged over the roughnesses of the terrain. Several approaches have been used.

1. Smith and Carson (1977) used the average geostrophic drag coefficient to define an effective roughness length.

$$u_i = \langle u \rangle = u_G$$

$$C_g^{\,eff} = \sum f_i C_{g,i}$$

Remember

$$u_G^{\,2} = C_G u_*^{\,2}$$

2. Taylor (1987) defined a definition for z_o that gives the correct spatial average wind profile rather than the correction shear stress.

If the wind velocity profiles in the spatial average are in equilibrium

$$\langle u(z)\rangle = \frac{1}{k}\left[\langle u_*\rangle \ln(z) - \langle u_* \ln(z_0)\rangle\right]$$

We can assess the roughness length by solving for the height where wind speed is zero. Arranging the equation yields:

$$\ln(z_{om}) = \langle \ln(z_0)\rangle = \frac{\langle u_* \ln(z_0)\rangle}{\langle u_*\rangle}$$

Note that the mean roughness length is not simply the mean of the roughness lengths of each path, but rather the weighted mean, associated with momentum transfer.

$$\ln(z_{0,m}) = \frac{\langle u_* \ln(z_{o,i})\rangle}{\langle u_*\rangle} \neq \langle \ln(z_{o,i})\rangle$$

In this case the wind profile is logarithmic but the apparent friction velocity is not equal to $\sqrt{\langle u_*^2\rangle}$. It is effectively a u* weighted estimate of zo.

$$\langle u(z)\rangle = \sqrt{\langle u_*^2\rangle} / k(\ln(z) - \ln(z_o^{\,eff}))$$

$$\langle \tau\rangle = \frac{\left[\langle u(z)^2\rangle + \langle u'^2\rangle\right]k^2}{\left[\ln(z) - \ln(z_o)\right]^2}$$

3. The third approach defines a mean effective roughness length that produces the mean shear stress(Mason, 1988). Mason develops an approach that performs weighting on the height of the blending height. They chose a blending height of L/200, where L is the horizontal scale of roughness variations.

$$\tau_G = \sum_i - f_i \overline{w'u'}_i = k^2 u(l_b)^2 \sum_i \frac{f_i}{(\ln(\frac{l_b}{z_{o,i}}))^2}$$

$$\left[\ln\left(\frac{l_b}{z_{o,eff}}\right)\right]^{-2} = \sum_i f_i / [\ln(l_b / z_{o,i})]^2$$

In this case $u(l_b)=\langle u \rangle$

Mason's method yields values that agree best with detailed numerical experiments.

Lengthscale	Zo grid	Zo method 1	Zo method 2	Zo method 3
1	0.82	0.35	0.16	0.77
100	0.43	0.35	-.16	0.38

4. A fourth method is proposed by Claussen.

The concept of the blending height has become powerful for parameterizing momentum transfer in complex terrain. It assumes that at sufficient heights, the effects of individual roughness elements are not seen, but the overall stress and velocity profile represesents the roughness of the whole area (Clausson, Wieringa). It has been proposed that fluxes be evaluated at the blending heights instead of the computing these fluxes with effective surface parameters, as the effective roughness lenghth of Wood and Mason (who extended their ideas to heat transfer). Claussen compared detailed model with the ideas of wood and mason

Aggregating Evaporation and Energy Transfer

Role of Spatial Variability on LE, due to spatial variability in model parameters and their spatial covariance with one another, can be investigated using simple Reynolds averaging rules, but for spatial rather than temporal variations. Here we assume that there is no horizontal advection across adjacent patches. Starting with the Penman-Monteith equation we have a function that is dependent on available energy, A, the vapor pressure deficit, D, the aerodynamic conductance, ga, the surface conductance, gs and the slope of the saturation vapor pressure curve, s, that is dependent on temperature:

$$\lambda E = \frac{sA + \rho C_p D g_a}{s + \gamma + \gamma(g_a / g_s)}$$

Substituting relations for instantaneous variables and averaging to assess the expected value we obtain:

$$E[\lambda E] = \frac{(\bar{s} + s')(\bar{A} + A') + \rho C_p (\bar{D} + D')(\bar{g}_a + g_a')}{(\bar{s} + s' + \gamma + \gamma(\bar{g}_a + g_a') / (\bar{g}_s + g_s')}$$

Rearrangement, yields mean and covariance terms:

$$E[\lambda E] = \frac{\bar{s}\bar{A} + \overline{s'A'} + \rho C_p(\bar{D}\bar{g}_a + \overline{D'g_a'})}{(\bar{s} + \gamma + \gamma(\bar{g}_a / \bar{g}_s + \overline{g_a r_s'}))}$$

The covariance terms can be reassessed in terms of their spatial variance and their correlation with the other covariant:

$$E[\lambda E] = \frac{\bar{s}\bar{A} + \overline{r_{As}\sigma_s\sigma_A} + \rho C_p(\bar{D}\bar{g}_a + \overline{r_{Dga}\sigma_D\sigma_{ga}})}{(\bar{s} + \gamma + \gamma(\bar{g}_a / \bar{g}_s + \overline{r_{gr}\sigma_{ga}\sigma_{rs}}))}$$

Aircraft transects can be used to explore spatial variance in the model parameters and the correlation between them. Obviously, if variables like g_a and D do not covary, such a term will drop out.

The weakness of this approach is that it does not consider interaction among 'pixels'; no advection is incorporated into this scheme. It only considers independent fluxes from the patchwork.

Other formal treatments of spatial variations in fluxes have been produced by (McNaughton, 1994) Raupach (1995), and Shuttleworth (1997). This key point is the need to weight variables by the flux.

For evaluating non-linear functions over space the flux must be conserved, so:

$$< R > \neq \sum w_i R_i$$

where w is the fractional component of each patch.

It is more appropriate to develop flux-weighted resistances in order to conserve material transfer

$$< R >= \frac{\sum F_i R_i}{\sum F_i}$$

Let's consider a region with 3 zones. The fluxes in zones 1 to 3 are 0.1, 0.5, and 0.4, summing to 1 and the resistances are 10, 50 and 40. If we average the component resistances we arrive at a value of 33.33 s/m. But the flux weighted resistance is 42 s/m

(0.1*10+0.5*50 +0.4*40). This simple numeric example clearly shows that using the average resistance will produce the wrong areally resistance and averaged flux.

McNaughton developed algorithms for assessing the role of spatial variance on the Penman Monteith equation. He defines an inverse conductance that is a function of proportional weighting factors

$$\frac{1}{R_a} = \sum_i \frac{w_i}{r_{a,i}}$$

Applying the concepts to evaporation

$$E = \frac{sR_aA + \rho\lambda D}{sR_a + (R_a + R_s)}$$

$$E_i = \frac{sr_{a,i}A + \rho\lambda D}{sr_{a,i} + (r_{a,i} + r_{s,i})}$$

We know that the mean grid averaged flux is the average of all the patch fluxes

$$< E >= \frac{\sum E_i}{n}$$

The challenge is to decode the proper resistances that must be used to evaluate the grid averaged evaporation flux.

$$R_a = \frac{R_d}{A} \sum_i \frac{w_i A_i r_{a,i}}{\Delta r_{a,i} + (r_{a,i} + r_{s,i})}$$

$$R_s = \frac{R_d}{A} \sum_i \frac{w_i A_i r_{s,i}}{\Delta r_{a,i} + (r_{a,i} + r_{s,i})}$$

The term Rd is defined as

$$R_d = \left[\sum_i \frac{w_i}{\Delta r_{a,i} + (r_{a,i} + r_{s,i})} \right]^{-1}$$

The term w is the fractional area of the patch in the grid.

This equation differs from the intuitive thought that the canopy stomatal resistance would equal the sum and average of the stomatal resistances of all the individual leaves.

Explicit calculations of spatial errors were recently evaluated using a surface energy balance model and a competition model between wet and dry plants using cellular automata.

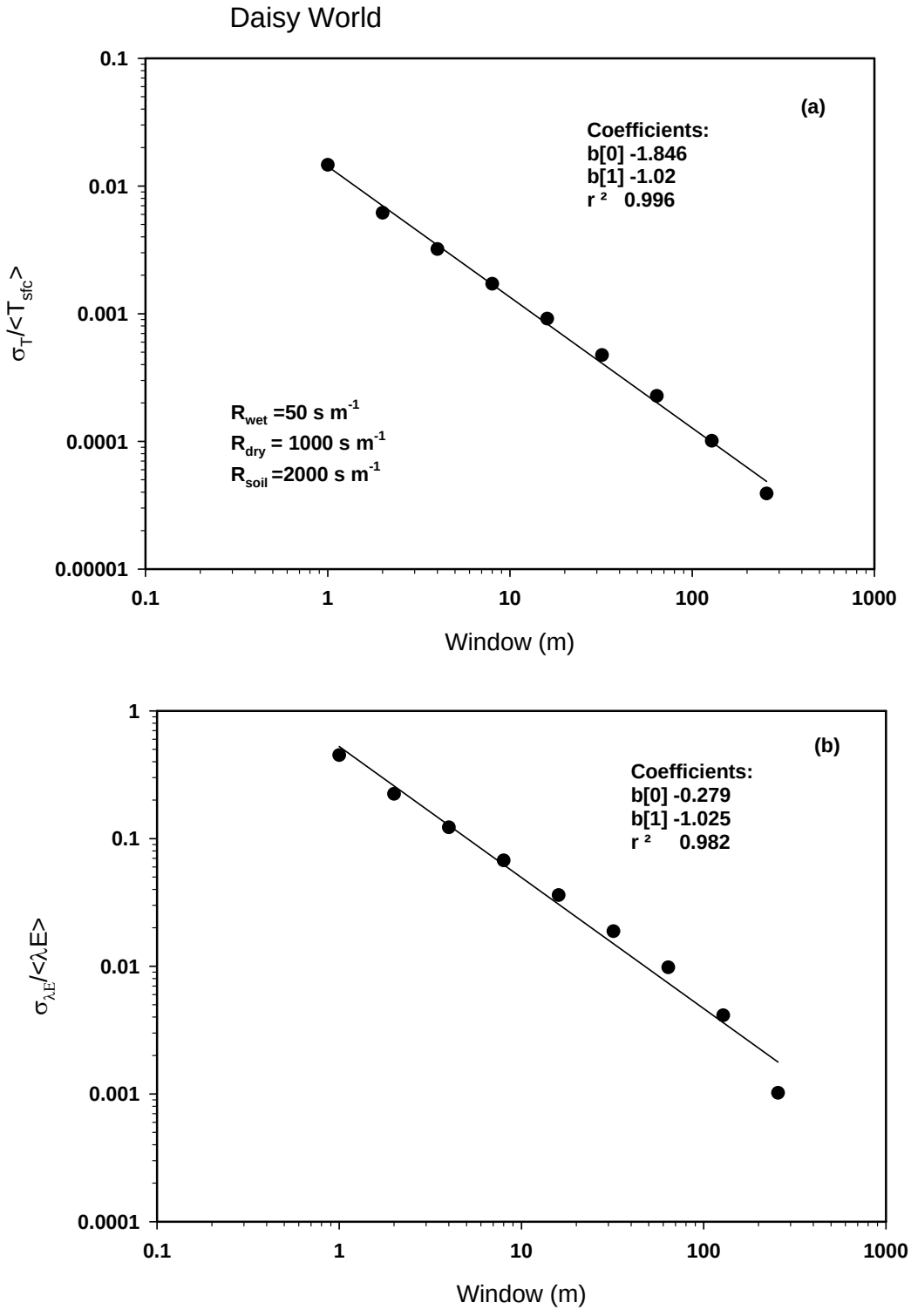

For the virtual landscapes simulated with 'Daisyworld', we observe large bias errors in estimating latent heat exchange (Figure 9a). On average, the mean latent heat flux is 154% greater than the expected value of latent heat exchange for the two-dimensional domain for the combination of variations in albedo and surface resistances of the wet and dry leaves. The magnitude of the relative bias error, however, is conditional

on the spatial coefficient of variation of latent heat exchange (Figure 9b), a reflection of the proportion and spatial variation of wet and dry 'daisies'. In general, the relative error term increases in magnitude in a non-linear fashion as the spatial coefficient of variation (c.v.) in λE increases. For highly heterogeneous landscapes (c.v approaching one), we observe that the relative bias error approaches 300%. For more homogeneous landscapes (c.v. ranging between 0 and 0.4), the relative bias error ranges between zero and 100%.

Bias errors associated with the evaluation of surface temperature are not as severe as those associated with λE. On average, we calculate a 3.5 K bias error in surface temperature, relative to its expected value (Figure 10a). This error is similar in magnitude with direct observations over heterogeneous land surfaces (Brunsell and Gillies, 2003; Kustas et al., 2003). Overall, the relative bias error increases from zero to 2.5% as the spatial coefficient of variation of surface temperature increases from zero to 2.5%. While a 4 K bias error represents a 1 to 2% relative error in terms of absolute temperature it has significant consequences on the assessment of the surface energy budget and latent heat exchange. This is because several components of the Penman-Monteith Equation are non-linear functions of surface temperature. For example, the long-wave emission is a function of surface temperature to the fourth power and the saturation vapor pressure is an exponential function of surface temperature. Consequently, a one percent error in surface temperature (at 300 K), for example, will produce a 4% error in long-wave energy emission.

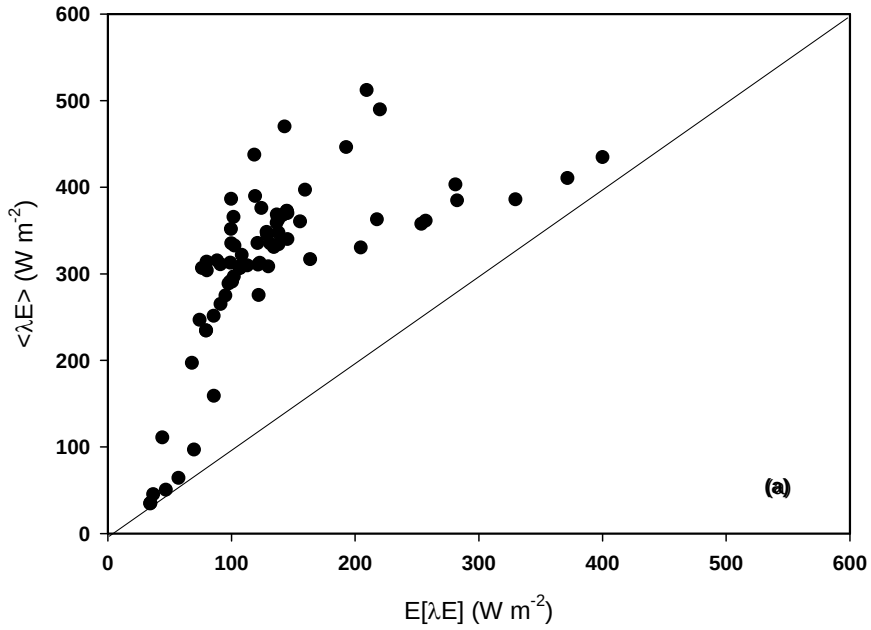

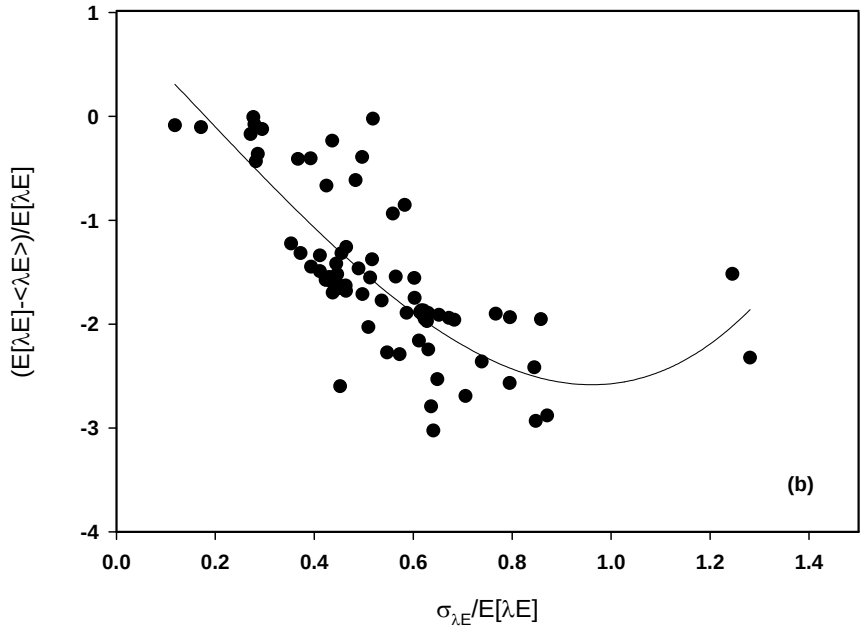

Advection

The advection of hot dry air can enhance evaporation downwind, while the advection of cool moist air can suppress evaporation downwind (McNaughton, 1994). So the distance from extreme edges can affect the areal averaged flux of heat, water and CO2 exchange

$$\frac{\partial c}{\partial t} + u\frac{\partial c}{\partial x} = -[\frac{\partial F}{\partial z} + \frac{\partial F}{\partial x}]$$

In the mid-80s, JR Philip, a pre-eminent theoretician evaluated the role of advection that would be imposed across a transition of vegetation with different stomatal conductances (Philip, 1987). His founding was fairly dramatic and indicated that advective effects would persist kilometers downwind from the edge of a vegetated transition.

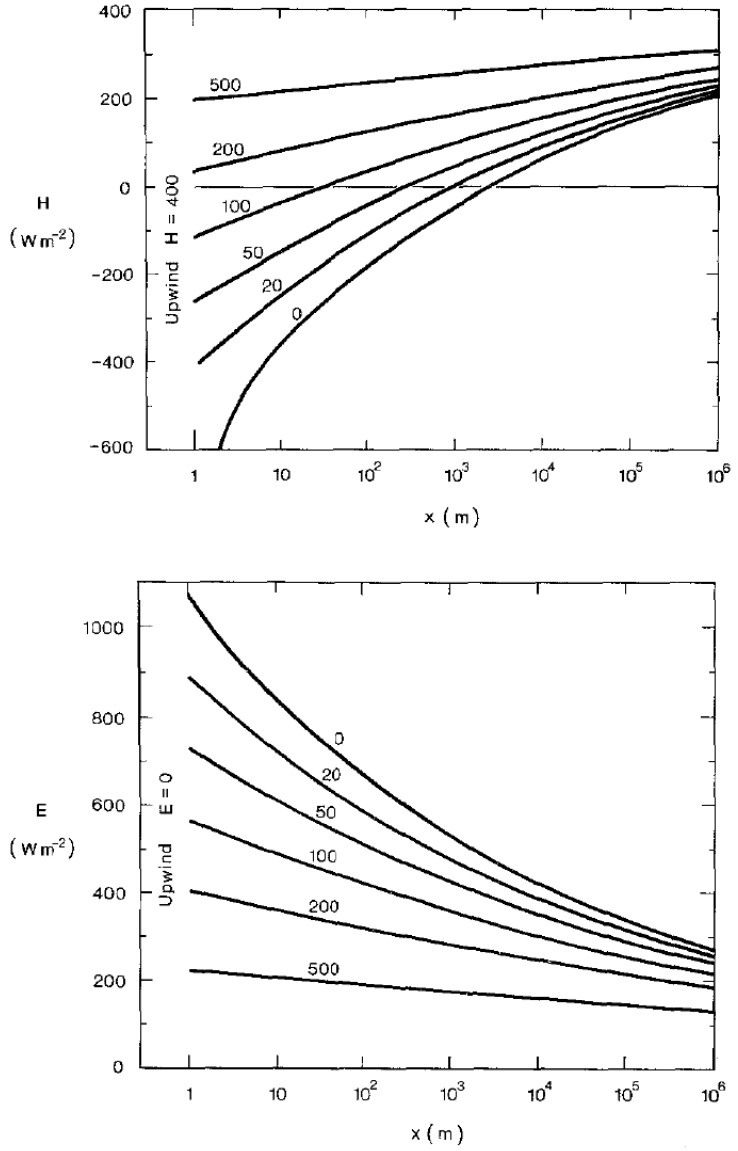

Figure 9 Analytical advection model (Philip, 1987)

To my mind this finding seemed artificial, and was a consequence of needing simple models to solve complex analytical differential equations; it ignored any feedbacks between stomatal conductance and vapor pressure deficits, for example. It also jived my personal observations growing up and working on farms. Look at corn fields next to a dry field, for example. One only sees stunted plants a few feet into the field, not kilometers. Complex feedbacks between stomata, advection and humidity feedbacks that are ignored in these computations and modulate the theory of Philip.

Table 1 Roles of feedbacks on advection potential

Process	No stomatal Feedback	With Stomatal Feedback
Advection hot, dry air	LE increases	Stomatal conductance decreases
		Increase in LE is modulated

A series of field studies ended up challenging the theme of Philip (Baldocchi and Rao, 1995; Brunet et al., 1994; Itier et al., 1994; Kroon and Debruin, 1993). The advection of dry air over actively transpiring vegetation may not necessarily increase evaporation if negative feedback causes stomatal closure, as stomatal closure would offset any potential increase in evaporation due to the advection of hot, dry air.

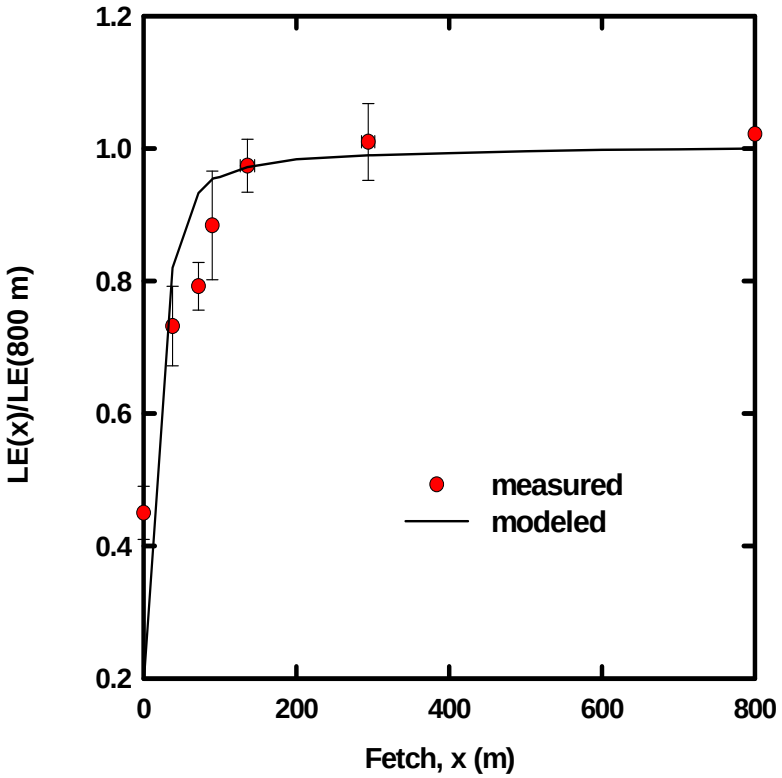

Figure 10 Field measurements over a potato field next to a desert and computations with a 2-dimensional second-order closure model that considered feedbacks between stomata and humidity deficits. (Baldocchi and Rao, 1995)

The magnitude of advective enhancement or repression of latent heat transfer depends, theoretically, on the **constituent patch size** and **stomatal feedbacks to the advected humidity deficit** (Raupach, 1991a). Klaassen (Klaassen, 1992) hypothesizes that the advective influence on latent heat transfer increases as the length scale of adjacent patches decreases. Whether or not this sensitivity of advection to patch size is significant can be debated. For one case, Klaassen (Klaassen, 1992)shows that the advective enhancement of λE is significant on relative terms (LE is enhanced by 5 to 20% as the length scale decreases from 10 km to 100 m). But in absolute terms, this evaporative enhancement may be considered trivial. Klaassen (1992) calculations indicate that advective effects alter λE by less than 10 W m^{-2} for the case studied. Raupach (Raupach, 1991a), in contrast of Philip (Philip, 1987), argues that **interfield** advection can be ignored if the horizontal scale of landscape patches is on the same scale as that of the convective boundary layer.

Application Problems

The role of landscape heterogeneity has been addressed numerous times by mesoscale modelers out of Roger Pielke's program at CSU.

Pielke et al (Pielke et al., 1998) summarize effects of surface homogeneities.

1. over homogeneous surfaces M-O theory is used to estimate fluxes of energy and momentum
2. when surface inhomogeneities are small (< 5 km), there effects are limited to the lower portion of the boundary layer. With small scale circulations aggregation methods are useful for evaluating fluxes
3. when spatial scale of surface heterogeneities is large (> 10 km), differential heating can be established and **mesoscale circulations** can be established, causing mesoscale circulations and fluxes to occur. These features can affect the amount and distribution of precipitation (Avissar and students). Specific patterns of vegetation will cause different thermal circulations and precipitation.

The types of land discontinuities that can establish mesoscale circulations include:

1) land-ocean (near Berkeley one can observe patterns of Kelvin Helholz waves that were perpendicular to one another at different levels. At a lower level a land-sea breeze was established and the cloud streaks were running north-south along the axis of the ocean. Higher level clouds seemed to have been caused by larger scale circulations and cloud streaks were running east-west.
2) Land-lake
3) Desert-irrigation
4) Forest-deforestation
5) Mountain flows

Roni Avissar, a former student of Piekle, has done considerable work using detailed mesoscale models, statistical-dynamic and Large eddy simulation models to evaluate the problem of landscape variability. In his recent review he identifies several schemes for evaluating surface heterogeneities and the land surface parameterization

1. mosaisic of tiles (Avissar and Pielke, 1989) in Land-Atmosphere Interactions Dynamics (LAID)
2. statistical-dynamic pdf approach (Avissar, 1992)
3. Large Eddy Simulation (LES) (Chen and Avissar)
4. Higher Order Closure SVAT model

Investigators generally assume that SVAT models can be scaled up to the macroscale with appropriate scaling factors, but often little attention is paid to non-linear responses with cloud formation and precipitation. In other words how do surface fluxes affect PBl

growth, cloud generation, landscape shadowing, convective rain and soil moisture and how these factors feedback on surface fluxes.

Avissar had developed an analytical method, FAST (Fourier Amplitude Sensititivity Test) to identify several factors as having a major influence on the estimation and distribution of energy exchange at the surface. These factors are:

1) surface wetness
2) surface roughtness
3) albedo
4) leaf area index
5) stomatal conductance

The spatial variability in these 5 factors needs to be considered to estimate the sub-rid and grid scale surface fluxes correctly. It is especially important if heterogeneity features are coherent and of large enough scale to generate surface level circulations., as they will tranport heat and moisture in the pbl and have prominent effects on cloud generation and convective precipitation (and light interception). Positive feedbacks can occur by replenishing soil moisture, if rain is significant.

Appendix A

Horst and Weil

Horst and Weil improved upon the work of Schuepp et al by considering the effects of atmospheric stability and the variation of wind speed with height. Their method, like the ones described so far is restricted to the atmospheric surface layer.

Horst and Weil first derive an equation that explains the footprint dependence upon crosswind location. They claim that the dependence of the flux footprint on crosswind location is identical to the crosswind concentration distribution for a unite surface point source.

The concentration at a point in space is a function of crosswind and vertical distribution functions and wind speed:

$$c(x,y,z) = \frac{D_y(x,y)D_z(x,z)}{U(x)}$$

Crosswind integrated concentration distribution function is defined from:

$$\int_{-\infty}^{\infty} D_y dy = 1$$

and the vertical concentration distribution function is defined from:

$$\int_0^\infty D_z dz = 1$$

The effective speed of the plume in the streamwise direction is:

$$U(x) = \int_0^\infty \bar{u}(z) D_z(x,z) dz$$

$$F_z = -K_c(z)\frac{\partial c}{\partial z} = -K_c \frac{D_y}{U}\frac{\partial D_z}{\partial z}$$

Integrating the flux over y, the cross-wind direction yields

$$\overline{F_y} = \int_{-\infty}^{\infty} -K_c(z)\frac{\partial c}{\partial z} dy$$

$$\overline{F_y} = -\frac{K_c}{U}\frac{\partial D_z}{\partial z}$$

$$F(x,y,z_m) = D_y(x,y)\overline{F_y}(x,z_m)$$

For a Gaussian plume:

$$D_y(x,y) = \exp\left(\frac{-y^2/2\sigma_y^2}{(2\pi)^{1/2}\sigma_y}\right)$$

Flux footprint Dependence on Measurement Height

$$\bar{u}\frac{\partial \overline{C_y}}{\partial x} = -\frac{\partial \overline{F_y}}{\partial z}$$

The cross-wind integrated footprint $\overline{f_y}$ is equal to the cross-wind integrated flux downwind of a unit surface point.

$$\overline{f_y}(x,z_m) \equiv \int_{-\infty}^{\infty} f(x,y,z_m) dy$$

It is also related to the cross wind integrated concentration distribution through the two-dimensional advection diffusion equation

$$\overline{f_y}(x,z_m) = -\int_0^{z_m} \bar{u}(z)\frac{\partial \overline{C_y}(x,z)}{\partial x}dz$$

$$\overline{C}_y(x,z) = \frac{D_z(x,z)}{U(x)} = \frac{AQ}{U(\bar{z})\bar{z}}\exp(-(\frac{z}{b\bar{z}})^r)$$

The mean height of a plume from a surface source is:

$$\bar{z}(x) = \frac{\int_0^\infty z\overline{D_y}(x,z)dz}{\int_0^\infty \overline{D_y}(x,z)dz}$$

The coefficient, r, is a shape factor. It equals 2 for the Gaussian plume model and 1 for exponential profile (e.g. Schuepp et al, 1990). The coefficients A and b are determined from Gamma functions:

$$A = r\Gamma(2/r)/\Gamma^2(1/r)$$

$$b = \Gamma(1/r)/\Gamma(2/r)$$

For the exponential model, A=b=1. For the Gaussian model:

$$A = \frac{2}{\pi}$$
$$b = \sqrt{\pi}$$
$$\bar{z} = \sqrt{\frac{2}{\pi}}\sigma_z$$

Horst and Weil use:

$$\overline{D_y}(x,z) = \frac{A}{U\bar{z}}\exp(-(\frac{z}{b\bar{z}})^r)$$

U is the effective speed of the plume advection.

$$U(x) = \frac{\int_0^\infty \bar{u}(z) D_y(x,z) dz}{\int_0^\infty D_y(x,z) dz}$$

$$\frac{d\bar{z}}{dx} = \frac{k^2}{[\ln(\frac{p\bar{z}}{z_0}) - \psi(\frac{p\bar{z}}{L})]\phi_c(\frac{p\bar{z}}{L})}$$

The coefficient p is 1.55, k is 0.40.

An approximation of the horizontally integrated function is:

$$\overline{f_y} \cong \frac{d\bar{z}}{dx}\frac{z_m}{\bar{z}^2}\frac{\overline{u(z_m)}}{u(c\bar{z})} A\exp(-(\frac{z_m}{b\bar{z}})^r)$$

$$U(x) = \bar{u}(c\bar{z})$$

$$\int_0^\infty D_z dz = 1$$

Integrating F over y

$$f(x,y,z_m) = D_y(x,y)\overline{F_y(x,z_m)}$$

cy and Fy are the cross-wind integrated concentration and fluxes.

$$\overline{u(z)} = \frac{u_*}{k}[\ln\frac{z}{z_0} + \psi(\frac{z}{L})]$$

At this stage Horst and Weil define a normalized, cross-wind integrated footprint

$$\Phi \equiv \frac{z_m F_y(x, z_m)}{Q d\bar{z} / dx}$$

$$\Phi = A \frac{z_m}{\bar{z}} \int_{z_0/\bar{z}}^{z_m/\bar{z}} \frac{\bar{u}(\zeta z)}{U(\bar{z})} (1 - r(\frac{\zeta}{b})^r + \frac{\bar{z}}{U(\bar{z})} \frac{dU}{d\bar{z}}) \exp(-(\frac{\zeta}{b})^r) d\zeta$$

$\zeta = z / \bar{z}$

U is the effective speed of the plume advection

$$\Phi \cong (\frac{z_m}{\bar{z}})^2 \frac{\overline{u(z_m)}}{U(\bar{z})} A \exp(-(\frac{z_m}{b\bar{z}})^r)$$

$$F = \frac{\Phi Q d\bar{z} / x}{z_m}$$

For the simplest case, a uniform surface emission (S_0), unlimited cross-wind extent and a finite upwind extent, x0, the footprint model is:

$$F(x_0, z_m) = S_o \int_0^{x_0} \frac{d(\bar{z} / z_m)}{d(x - x')} \Phi(\bar{z} / z_m) d(x - x')$$

The term x-x' represents the streamwise separation between the measurement location and the location of the emission.

Schmid

1. Discriminates between footprint and source area of diffusive scalars and footprint and source area of scalar fluxes.

The scalar footprint relates to the field of view for the scalar instrument, such as a thermometer. The flux footprint relates to the field of view for a flux measurement.

Studies by Schuepp, Leclerc, Horst and Weil, Gash define a source weight function, often called a footprint.

The source area is the integral of the source weight function or footprint, with space.

Schmid defines the problem of relating the spatial distribution of sources and its measurement at a given height into two classes. The source weight function or 'footprint' and the source area. The source area is the integral of the source weight function over some domain.
There is another nuance. Some papers deal with the diffusion of scalars and their concentrations other determine fluxes. Schmid distinguishes between flux and concentration footprints.

Source area for a passive scalar

$$C(x, y, z_m) = Q_{c,u} \frac{D_y(x, y) D_z(x, z)}{U(x)}$$

Q is point source strength.

$$f_c(x, y, z_m - z_0) = \frac{C(x, y, z_m)}{Q_{c,u}} = \frac{D_y(x, y) D_z(x, z_m)}{u(x)}$$

$$\overline{D_y}(x, z) = \frac{A}{\overline{U} z} \exp(-(\frac{z}{\overline{=}})^r)$$

Source area for a scalar flux

Schmid comments that some of the pioneering papers refer to concentration and other refer to flux.

$$F(r) = \int_{-\infty}^{x} S(r') f(r - r') dr'$$

a. concentration footprint.

$$F(x_m, y_m, z_m) = \int_{-\infty}^{\infty} \int_{-\infty}^{\infty} S(x', y', z_0) f(x_m - x', y_m - y', z_m - z_0) dy' dx'$$

Schmid (Schmid, 1994) states that the theory of Horst and Weil define a scalar concentration source weight function, as their derivation starts with a diffusion equation for C.

Later HW also define a flux footprint

$$F_z = -K_c(z)\frac{\partial c}{\partial z} = -K_c Q_{c,u}\frac{D_y}{U}\frac{\partial D_z}{\partial z} = D_y(x,y)\overline{F^y(x,z)}$$

Dy is the cross wind distribution function

References:

Avissar, R. 1992. Conceptual aspects of a statistical-dynamical approach to represent landscape subgrid scale heterogeneities in atmospheric models. Journal of Geophysical Research. 97, 2729-2742.

Avissar, R. and R. Piekle. 1989. Parameterization of heterogeneous land surface for atmospheric numerical models and its impact on regional meteorology. Monthly Weather Review. 117, 2113.

Avissar, R. 1998. Which type of soil-vegetation-atmosphere transfer scheme is needed for general circulation models: a proposal for a higher order scheme. J. Hydrology. 212-213: 136-154.

Belcher, S.E. and JCR Hunt. 1998. Turbulent flow over hills and waves. Annual review of Fluid Mechanics. 30, 507-538.

Mason, P.J. 1988. The formation of areally-averaged roughness lengths. Quarterly Journal of the Royal Meteorological Society. 114, 399-420.

McNaughton, KG. 1994. Effective stomatal and boundary layer resistances for heterogeneous surfaces. Plant, cell and Environment. 17, 1061-1068.

McNaughton, KG. 1989. Regional interactions between canopies and the atmosphere. In: Plant Canopies: Their Growth, Form and Function. Cambridge. Russel, G, Marshall, B and Jarvis, PG, eds.

Pielke, R.A. 2001. Influence of the spatial distribution of vegetation and soils on the prediction of cumulus convective rainfall. *Reviews of Geophysics*. 39, 151-177.

Schmid, HP and CR Lloyd. 1999. Spatial representativeness and the location bias of flux footprints over inhomogeneous areas. Agricultural and Forest Meteorology. 93, 195-209.

EndNote References

Amiro, B.D., 1998. Footprint climatologies for evapotranspiration in a boreal catchment. Agricultural and Forest Meteorology, 90(3): 195-201.

Avissar, R., 1995. Scaling of land-atmosphere interactions-an atmospheric modeling perspective. Hydrological Processes, 9: 679-695.

Avissar, R. and Pielke, R., 1989. A PARAMETERIZATION OF HETEROGENEOUS LAND SURFACES FOR ATMOSPHERIC NUMERICAL-MODELS AND ITS IMPACT ON REGIONAL METEOROLOGY. Monthly Weather Review, 117: 2113-2136.

Avissar, R. and Verstraete, M.M., 1990. The Representation of Continental Surface Processes in Atmospheric Models. Reviews of Geophysics, 28(1): 35-52.

Baldocchi, D.D., 1997. Flux footprints under forest canopies. Boundary Layer Meteorology, 85: 273-292.

Baldocchi, D.D., Krebs, T. and Leclerc, M.Y., 2005. 'Wet/Dry Daisyworld': A Conceptual Tool for Quantifying Sub-Grid Variability of Energy Fluxes over Heterogeneous Landscapes. Tellus, 57: 175-188.

Baldocchi, D.D. and Rao, K.S., 1995. Intra-field variability of scalar flux densities across a transition between a desert and an irrigated potato Advection field. Boundary Layer Meterology., 76.: 109-136.

Brunet, Y., Finnigan, J.J. and Raupach, M., 1994. A wind tunnel study of air flow in waving wheat-single point velocity statistics. Boundary Layer Meteorology, 70: 95-132.

Brunsell, N.A. and Gillies, R.R., 2003. Scale issues in land-atmosphere interactions: implications for remote sensing of the surface energy balance. Agricultural and Forest Meteorology, 117(3-4): 203-221.

Chasmer, L. et al., 2011. Characterizing vegetation structural and topographic characteristics sampled by eddy covariance within two mature aspen stands using lidar and a flux footprint model: Scaling to MODIS. J. Geophys. Res., 116(G2): G02026.

Claussen, M., 1991. ESTIMATION OF AREALLY-AVERAGED SURFACE FLUXES. Boundary-Layer Meteorology, 54(4): 387-410.

Crawford, T., Dobosy, R., McMillen, R., Vogel, C. and Hicks, B., 1996. Air-surface exchange measurement in heterogeneous regions: Extending tower observations with spatial structure observed from small aircraft. Global Change Biol, 2: 275-285.

Crawford, T.L., Mcmillen, R.T., Meyers, T.P. and Hicks, B.B., 1993. Spatial and Temporal Variability of Heat, Water-Vapor, Carbon-Dioxide, and Momentum Air-Sea Exchange in a Coastal Environment. Journal of Geophysical Research-Atmospheres, 98(D7): 12869-12880.

Desjardins, R.L., Brach, E.J., Alvo, P. and Schuepp, P.H., 1982. Aircraft Monitoring of Surface Carbon-Dioxide Exchange. Science, 216(4547): 733-735.

Desjardins, R.L. et al., 1997. Scaling up flux measurements for the boreal forest using aircraft-tower combinations. Journal of Geophysical Research, 102: 29125-29134.

Detto, M., Katul, G., Mancini, M., Montaldo, N. and Albertson, J.D., 2008. Surface heterogeneity and its signature in higher-order scalar similarity relationships. Agricultural and Forest Meteorology, 148(6-7): 902-916.

Dolman, A.J. et al., 2006. The CarboEurope regional experiment strategy. Bulletin of the American Meteorological Society, 87(10): 1367-1379.

Doran, J.C. et al., 1992. The Boardman Regional Flux Experiment. Bulletin of the American Meteorological. Society., 73: 1785-1795.

Foken, T. and Leclerc, M.Y., 2004. Methods and limitations in validation of footprint models. Agricultural and Forest Meteorology, 127(3-4): 223-234.

Gash, J.H.C. et al., 1989. Micrometeorological Measurements in Les-Landes Forest During Hapex-Mobilhy. Agricultural and Forest Meteorology, 46(1-2): 131-147.

Gockede, M., Rebmann, C. and Foken, T., 2004. A combination of quality assessment tools for eddy covariance measurements with footprint modelling for the characterisation of complex sites. Agricultural and Forest Meteorology, 127(3-4): 175-188.

Horst, T.W. and Weil, J.C., 1992. Footprint Estimation for Scalar Flux Measurements in the Atmospheric Surface-Layer. Boundary-Layer Meteorology, 59(3): 279-296.

Hsieh, C.-I., Katul, G. and Chi, T.-w., 2000a. An approximate analytical model for footprint estimation of scalar fluxes in thermally stratified atmospheric flows. Advances in Water Resources, 23(7): 765-772.

Hsieh, C.I., Katul, G. and Chi, T., 2000b. An approximate analytical model for footprint estimation of scaler fluxes in thermally stratified atmospheric flows. Advances in Water Resources, 23(7): 765-772.

Itier, B., Brunet, Y., McAneney, K.J. and Lagouarde, J.P., 1994. Downwind Evolution of Scalar Fluxes and Surface-Resistance under Conditions of Local Advection .1. A Reappraisal of Boundary-Conditions. Agricultural and Forest Meteorology, 71(3-4): 211-225.

Kim, J. et al., 2006. Upscaling fluxes from tower to landscape: Overlaying flux footprints on high-resolution (IKONOS) images of vegetation cover. Agricultural and Forest Meteorology

Advances in Surface-Atmosphere Exchange - A Tribute to Marv Wesely, 136(3-4): 132-146.

Klaassen, W., 1992. Average Fluxes from Heterogeneous Vegetated Regions. Boundary-Layer Meteorology, 58(4): 329-354.

Klaassen, W. and Claussen, M., 1995. Landscape variability and surface flux parameterization in climate models. Agricultural and Forest Meteorology, 73(3-4): 181-188.

Kljun, N., Kastner-Klein, P., Fedorovich, E. and Rotach, M.W., 2004. Evaluation of Lagrangian footprint model using data from wind tunnel convective boundary layer. Agricultural and Forest Meteorology, 127(3-4): 189-201.

Kroon, L.J.M. and Debruin, H.A.R., 1993. Atmosphere Vegetation Interaction in Local Advection Conditions - Effect of Lower Boundary-Conditions. Agricultural and Forest Meteorology, 64(1-2): 1-28.

Kustas, W.P., Norman, J.M., Anderson, M.C. and French, A.N., 2003. Estimating

subpixel surface temperatures and energy fluxes from the vegetation index-radiometric temperature relationship. Remote Sensing of Environment, 85(4): 429-440.

Leclerc, M.Y. et al., 2003a. Impact of non-local advection on flux footprints over a tall forest canopy: a tracer flux experiment. Agricultural and Forest Meteorology, 115(1-2): 19-30.

Leclerc, M.Y., Meskhidze, N. and Finn, D., 2003b. Comparison between measured tracer fluxes and footprint model predictions over a homogeneous canopy of intermediate roughness. Agricultural and Forest Meteorology, 117(3-4): 145-158.

Leclerc, M.Y. and Thurtell, G.W., 1990. Footprint prediction of scalar fluxes using a Markovian analysis. Boundary Layer Meteorology, 52: 247-258.

Levin, S.A., 1992. The problem of pattern and scale in ecology. Ecology, 73: 1943-1967.

Mason, P.J., 1988. THE FORMATION OF AREALLY-AVERAGED ROUGHNESS LENGTHS. Quarterly Journal of the Royal Meteorological Society, 114(480): 399-420.

McNaughton, K.G., 1994. Effective stomatal and boundary-layer resistances of heterogeneous surfaces. Plant Cell and Environment, 17: 1061-1068.

Miglietta, F., Gioli, B., Hutjes, R.W.A. and Reichstein, M., 2007. Net regional ecosystem CO_2 exchange from airborne and ground-based eddy covariance, land-use maps and weather observations. Global Change Biology, 13(3): 548-560.

Philip, J.R., 1987. Advection, Evaporation, and Surface-Resistance. Irrigation Science, 8(2): 101-114.

Pielke, R.A. et al., 1998. Interactions between the atmosphere and terrestrial ecosystems: influence on weather and climate. Global Change Biol, 4(5): 461-475.

Rao, K.S., Wyngaard, J.C. and Cote, O.R., 1974. Structure of 2-Dimensional Internal Boundary-Layer over a Sudden Change of Surface-Roughness. Journal of the Atmospheric Sciences, 31(3): 738-746.

Raupach, M.R., 1991a. Vegetation-Atmosphere Interaction in Homogeneous and Heterogeneous Terrain - Some Implications of Mixed-Layer Dynamics. Vegetatio, 91(1-2): 105-120.

Raupach, M.R., 1991b. Vegetation-atmosphere interaction in homogeneous and heterogeneous terrain: some implications of mixed-layer dynamics. Plant Ecology, 91(1 - 2): 105-120.

Raupach, M.R., 1995. Vegetation-atmosphere interaction and surface conductance at leaf, canopy and regional scales. Agricultural and Forest Meteorology, 73(3-4): 151-179.

Raupach, M.R., 1998. Influences of local feedbacks on land-air exchanges of energy and carbon. Global Change Biology, 4(5): 477-494.

Raupach, M.R. and Finnigan, J.J., 1995. Scale issues in boundary layer meteorology-surface energy balances in heterogeneous terrain. Hydrological Processes, 9: 589-612.

Rebmann, C. et al., 2005. Quality analysis applied on eddy covariance measurements at complex forest sites using footprint modelling. Theoretical and Applied Climatology, 80(2 - 4): 121-141.

Schmid, H.P., 1994. SOURCE AREAS FOR SCALARS AND SCALAR FLUXES. Boundary Layer Meteorology, 67: 293-318.

Schmid, H.P., 2002. Footprint modeling for vegetation atmosphere exchange studies: a review and perspective. Agricultural and Forest Meteorology, 113(1-4): 159-183.

Schuepp, P., Leclerc, M.Y., Macpherson, I.J. and Desjardins, R.L., 1990. Footprint prediction of scalar fluxes from analytical solutions of the diffusion equation. Boundary Layer Meteorology, 50: 353-373.

Sellers, P.J. and Hall, F.G., 1992. Fife in 1992 - Results, Scientific Gains, and Future-Research Directions. Journal of Geophysical Research-Atmospheres, 97(D17): 19091-19109.

Sellers, P.J. et al., 1997. Boreas in 1997: Scientific results; experimental overview and future directions. Journal of Geophysical Research., 102: 28731- 28770.

Shuttleworth, W.J., 1991. Insight from Large-Scale Observational Studies of Land Atmosphere Interactions. Surveys in Geophysics, 12(1-3): 3-30.

Vesala, T. et al., 2008. Flux and concentration footprint modelling: State of the art. Environmental Pollution, 152(3): 653-666.